Thermal Unfolding and Refolding Trajectory of Single Calmodulin Proteins by Plasmonic Optical Tweezers

Cuifeng Ying,[1] **Edona Karakaçi**,[2] **Esteban Bermúdez-Ureña**,[2] **Reuven Gordon**,[3] **Michael Mayer** [2]

1. Advanced Optics and Photonics Lab, Department of Engineering, Nottingham Trent University, United Kingdom
2. Adolphe Merkle Institute, University of Fribourg, Chemin des Verdiers 4, CH-1700 Fribourg, Switzerland.
3. Department of Electrical and Computer Engineering, University of Victoria, Victoria, British Columbia V8P 5C2, Canada

Email: cuifeng.ying@ntu.ac.uk

Conformational dynamics are critical for the function of many proteins. Studying conformational changes of proteins in response to external stimuli is therefore essential for determining their function in human cells, and their contribution to both health and disease. Established approaches to monitor conformational changes of proteins require modification of the target proteins, either by attaching fluorophores (or other labels) to conduct single-molecule fluorescence resonance energy transfer (smFRET) experiments or by attaching molecular tethers to conduct single-molecule force spectroscopy (smFS) experiments. A recently developed approach in the nanophotonics field, plasmonic optical tweezers, has demonstrated the potential to trap unlabeled, nanoscale objects and monitor the behavior of these objects over time [1, 2]. This work reports the first thermal unfolding and refolding trajectory of a single protein by using the double-nanohole (DNH) plasmonic optical tweezer (Fig. 1a-d) [3]. We trapped single calmodulin proteins from solution and monitored the conformational changes of proteins from changes in transmission, at the same time tuning the temperature in the trapping site by adjusting the laser power (Fig.1e,f). We demonstrated that single *apo*-calmodulin thermally unfolds and refolds in steps by conformational fluctuations of individual protein domains (Fig. 1g, h). The conformational changes of individual calmodulin domains result in readily detectable changes in transmission for as long as two hours without possible limitations by photobleaching of fluorescent labels or contamination of scanning probe tips for force spectroscopy. The results agree with smFS and suggest general utility for single-molecule protein folding studies [4]. We expect that this approach will rapidly establish itself in the field of conformational protein dynamics because research groups without expertise in site-directed mutagenesis and chemical modification of single proteins will be able to carry out detailed biophysical studies on conformational dynamics.

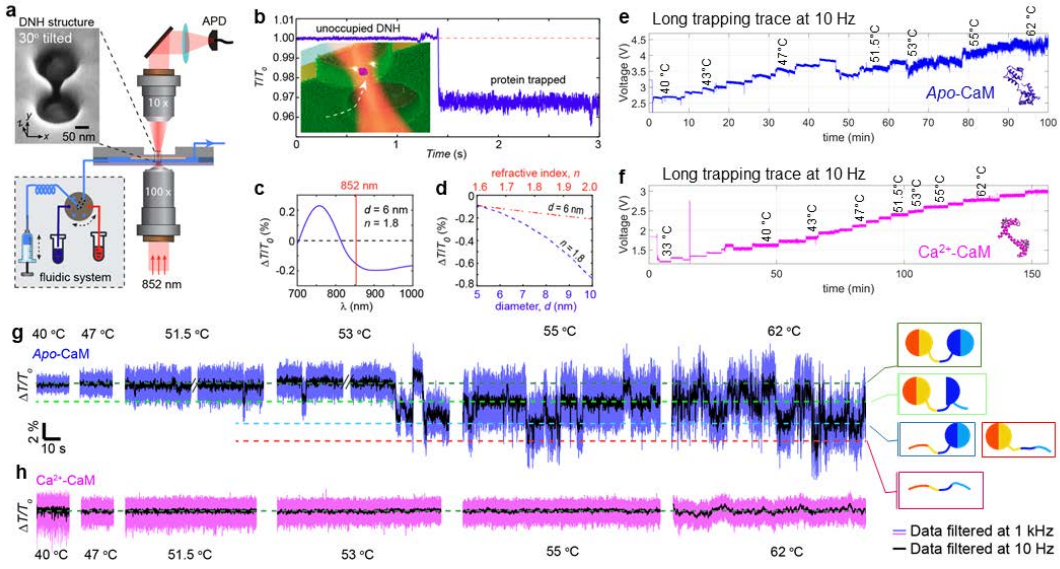

Fig. 1 a, Schematic of the plasmonic optical tweezer platform. The scanning electron microscopy (SEM) image shows a plasmonic double-nanohole (DNH) structure in a 100 nm thick film of gold. **b**, Experimental transmission time trace for a protein being trapped in a DNH structure. Here T_0 is the baseline from the light transmission of the empty DNH. The inset cartoon illustrates the polymer coating of the DNH samples with a protein trapped in the gap. **c**, Simulated change in transmission, $\Delta T/T_0$, as a function of wavelength after trapping a particle with a diameter, d, of 6 nm and a refractive index, n, of 1.8. **d**, Simulated dependence of $\Delta T/T_0$ (at λ = 852 nm) on particle size (blue, n = 1.8) and refractive index (red, d = 6). **e, f** Transmission through a DNH with either a trapped **e**, *apo*-CaM or **f**, Ca^{2+}-CaM in response to stepwise increases in temperature. **g, h,** magnified transmission trace for **g**, *apo*-CaM or **h**, Ca^{2+}-CaM at different temperatures from panels e and f. Four dashed lines represent three folding states of CaM that are identified in the transmission signal. The corresponding structures are illustrated as cartoons on the right. The cartoons are adapted from Ref [4].

References

[1] Juan, M. L.; Gordon, R.; Pang, Y.; Eftekhari, F.; Quidant, R. 2009, *Nat. Phys.* 5, 915–919
[2] Pang, Y.; Gordon, R. 2012, *Nano Lett.* 12, 402–406.
[3] Ying, C.; Karakaci, E.; Bermudez-Urena, E.; Ianiro, A.; Foster, C.; Awasthi, S.; Guha, A.; Bryan, L.; List, J.; Balog, S. 2021, *arXiv Prepr,* arXiv2107.06407.
[4] Stigler, J.; Ziegler, F.; Gieseke, A.; Gebhardt, J. C. M.; Rief, M. 2011, *Science* 334, 512–516.

Polarization dependence of double nanohole tweezers for localization and orientation

Ghazal Hajisalem[1,2], **Michael Dobinson**[1,2], **Zohreh Sharifi**[1,2], **Jon Eby**[1,2], **and Reuven Gordon**[1,2]

1. Department of Electrical and Computer Engineering, University of Victoria, Victoria, British Columbia V8P 5C2, Canada
2. Centre for Advanced Materials and Related Technology (CAMTEC), University of Victoria, Victoria, British Columbia V8P 5C2, Canada
E-mail: ghazalh@uvic.ca

Double nanohole (DNH) optical tweezers localize the high field enhancement in the gap regions as small as 10 nm allowing for trapping and analyzing proteins [1]. However, using a DNH as a trapping site requires localizing it on the substrate by complicated methods such as scanning electron microscope (SEM). Here we investigate the polarization dependence of DNHs using the optical trapping setup and show that can be used to identify a DNH in the trapping site. We also show that the polarization response can determine orientation of DNHs on a substrate. The polarization dependence analyzes of DNHs allows for using DNH optical tweezers without the need for SEM or other expensive and complicated methods and make it more accessible without access to such facilities.

Figure 1(a) shows a schematic of an optical tweezer setup [2] we used in this measurement. Here a 980 nm continuous wave diode laser beam was collimated, expanded, and focused through a 100× microscope objective into a nanoaperture (in the sample substrate). The transmitted signal was collected by a 10× microscope objective and measured by an avalanche photodiode (APD – Thorlabs, APD120A). The polarization direction of the laser beam was rotated in steps by a half-wave plate (HWP) in front of the laser. Figure 1(b) shows SEM images of nanoapertures in a substrate: two DNHs apertures (labeled as "DNH 1" and "DNH 2") with their axes normal in respect to each other and a single nanohole (labeled as "SNH 1"). Nanoapertures in gold on glass substrate were fabricated by using the colloidal lithography method [3]. Figure 1(c) shows the polarization dependence of the laser transmission signal through the DNHs and the SNH apertures shown in (b). Sinus lines were fitted to the measured data in each plot. The DNHs with normal axes in respect to each other showed opposite transmission response of the laser beam, allowing for determining the orientation of the DNHs in respect to each other and without having their SEM images. The polarization response of DNHs was much stronger than the SNH, allowing for identifying the DNHs from the SNH. The SNH is expected to not show any polarization dependence. Our measurements with SNHs and without a sample showed similar slight polarization dependence that we believe this was mainly coming from the polarization dependence of the setup. We showed that using the polarization dependence analysis allows for identifying DNHs in-site and without using complicated imaging methods such as SEM. Also, it can be used to determine their orientation, making the high quality optical trapping using DNH structures accessible to a broad scientific community.

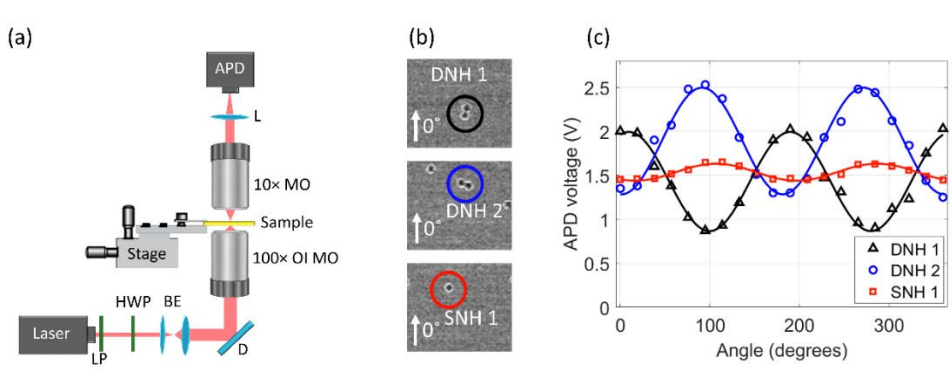

Fig. 1 (a) Schematic of an optical tweezer setup: linear polarizer (LP), half-wave plate (HWP), beam expander (BE), dichroic mirror (D), 100 × oil immersion microscope objective (100 × OI MO), piezo stage (stage), 10 × microscope objective (10 ×MO), lens (L), and avalanche photodetector (APD). (b) SEM images of DNHs with their axes normal in respect to each other and an SEM image of a SNH. (c) Polarization dependence of the laser transmission of the apertures shown in (b). The DNHs with normal axes in respect to each other show opposite transmission response of the laser beam. The SNH polarization dependent response was much weaker than the DNHs responses.

References

[1] S. Wheaton and R. Gordon, "Single molecule protein sizing in double nano-hole optical tweezers," in Optical Trapping Applications, (Optical Society of America, 2015), pp. OtM3E–5.
[2] G. Hajisalem, E. Babaei, M. Dobinson, S. Iwamoto, Z. Sharifi, J. Eby, M. Synakewicz, L. S. Itzhaki, and R. Gordon, "Accessible high-performance double nanohole tweezers," Opt. Express 30(3), 3760–3769 (2022).
[3] A. L. Ravindranath, M. Seyed Shariatdoust, S. Mathew, and R. Gordon, "Colloidal lithography double-nanohole optical trapping of nanoparticles and proteins," Opt. Express 27(11), 16184–16194 (2019).

Manipulating and characterizing individual bio-particles in nanochannels

Gabriel Schnoering[a], Christian Höller[a], Hadi Eghlidi[a], Maarit Suomalainen[b], Urs F. Greber[b] and Dimos Poulikakos[a]

[a] Laboratory of Thermodynamics in Emerging Technologies, ETH Zurich, Sonneggstrasse 3, Zurich, Switzerland
[b] Institute of Molecular Life Sciences, University of Zurich, Zurich, Switzerland
e-mail: schngabr@ethz.ch

Manipulation of matter at the nanoscale and at the single entity level is of utmost importance in a large variety of fields ranging from basic sciences to biology and medicine. It is particularly appealing in order to develop an understanding of complex entities such as viruses, characterize them and assert their biological/chemical function when interacting with other entities in biological fluids. Modern and successful approaches mostly exploit configurations where a strong gradient of field provides a stable attracting potential in space, generated by tightly focused propagating fields or in the near field of antennas. However, due to the volume dependence of their polarizability, sub-100 nm nano-objects require strong and potentially harmful field intensities.

In this work, we transport individual nano-objects in biological level ionic solutions to select locations in on-chip nanochannels using dielectrophoretic nanovalves [1]. In-between two such nanovalves the nano-object is confined and we study its judiciously restricted thermal motion [2]. The confined particle dynamics is analyzed and provides important properties at the individual nano-object level such as the diffusion coefficient, hydrodynamic diameter, trap stiffness and electrical conductivity of the individual particles. We show the versatility of our system by assessing the properties of polystyrene nanospheres, conjugated polymer nanoparticles and adenoviruses.

The collaborative effect of the applied alternating current (AC) electric field between nanoelectrodes and a designed and fabricated nanochannel topography locally amplifies the near-field gradient of a RF field, forming together a harmonic trap between a nanovalves system with no-moving-parts effective for various dielectric nanoparticles. This work is an important advancement in manipulating and characterizing individual nano-objects in biologically relevant ionic solutions, including novel medical nanomaterials, or specific viruses.

References

[1] Eberle, P.; Höller, C.; Müller, P.; Suomalainen, M.; Greber, U. F.; Eghlidi, H.; Poulikakos, D. Single Entity Resolution Valving of Nanoscopic Species in Liquids. *Nat. Nanotechnol.* 2018, 13 (7), 578–582.

[2] Höller, C; Schnoering, G; Eghlidi, H; Suomalainen, M; Greber, U; Poulikakos, D. On-chip transporting arresting and characterizing individual nano-objects in biological ionic liquids. *Science Advances*, In press

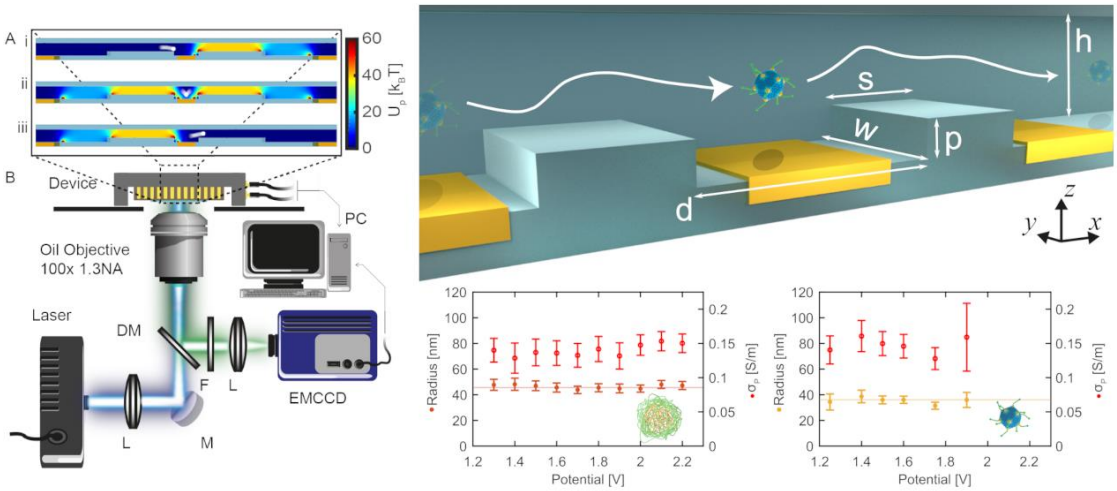

Figure 1. Individual nano-objects are transported through an on-chip nanochannel and arrested between two nanovalves. The restricted motion is recorded and analyzed via its spectral density and from which the radius and conductivity of individual particles are obtained at different electrodes potential. This is performed for individual nanoparticles such as conjugated polymer nanoparticles and adenoviruses in high-ionic environments.

Photothermal expansion nanoscopy of the strong coupling between a patch nanoantenna and a semiconductor quantum well

Simone Sotgiu[1], Mario Malerba[2], Leonetta Baldassarre[1,3], Valeria Giliberti[3], Lianhe Li[4], A. Giles Davies[4], Edmund H. Linfield[4], Andrea Schirato[5,6], Alessandro Alabastri[7], Mathieu Jeannin[2], Jean-Michel Manceau[2], Raffaele Colombelli[2] and Michele Ortolani [1,3]

1. Department of Physics, Sapienza University of Rome, 00185 Rome, Italy
2. Centre de Nanosciences et de Nanotechnologies, Université Paris-Saclay, 91405 Orsay, France
3. Istituto Italiano di Tecnologia, Center for Life Nano- & Neuro-Science, I-00161 Rome, Italy
4. School of Electronic and Electrical Engineering, University of Leeds, Woodhouse Lane, Leeds LS2 9JT, United Kingdom
5. Department of Physics - Politecnico di Milano, I-20133 Milan, Italy
6. Istituto Italiano di Tecnologia, I-16163, Genoa, Italy
7. Rice University, Houston (TX), U.S.A.

E-mail: simone.sotgiu@uniroma1.it

The strong light-matter coupling is an exotic phenomenon of interest not only for basic physics, but also because of its potential for improving optoelectronic devices. Conduction-band electrons in semiconductor quantum wells (QWs) display narrow intersubband (ISB) transitions in the far- and mid-IR that can couple to the optical resonances of metallic nanoantennas. Strong light-matter coupling appears in the form of new mixed light-matter eigenmodes, called intersubband cavity polaritons [1]. The signature of this regime is the characteristic anti-crossing of the "light" and "matter" excitations when the two resonances spectrally overlap.

In the mid-IR, cavity electrodynamics phenomena are best explored using metallic antennas, one of the simplest layout being the metal-insulator-metal (MIM) patch antenna, as metal losses are acceptable and optical confinement can be record-high. Mid-IR spectroscopy measurements in the far-field however require arrays made up of hundreds of resonators to obtain a good signal-to-noise ratio. Furthermore, the core of the architecture – the active region where the light-matter interaction takes part – is concealed by the metal and mostly accessible to direct near-field nanoscopy with scanning probes (e.g. scattering SNOM).

Here we present a novel approach to single resonator spectroscopy based on photothermal induced resonance (PTIR) expansion nanoscopy with a contact-mode scanning probe, alternative to SNOM techniques [2], capable *not only* of detecting the spectral response of a single MIM cavity in the mid-IR range, *but also* of mapping the electromagnetic fields buried within with deep-subwavelength resolution.

We achieve this by inserting in a MIM resonator a 100-nm-thick "probe" layer of (IR-transparent) polyethylene along with a single heavily-doped epitaxially-grown QW (Fig. 1a). By shining a tunable mid-IR quantum cascade laser on the system, the cavity absorbs energy at its resonance wavelengths.

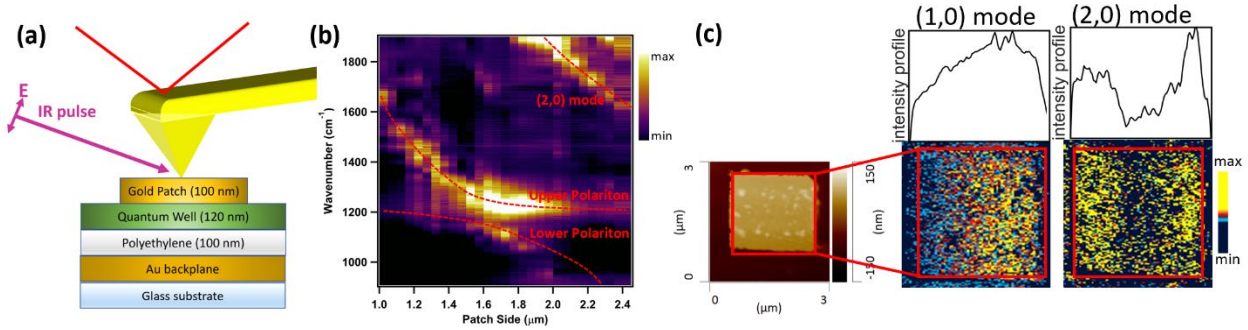

Fig. 1 (a) Scheme of the sample and experimental set-up. (b) Color plot of the spectra acquired as a function of the patch lateral side. (c) IR absorption maps acquired at the first and second resonance order.

In contrast to usual PTIR nanoscopy, the polymer here is not the object of investigation. It operates instead as a thermal expansion *transducer* transforming the light absorbed by the cavity into a vertical displacement, measured by the scanning probe. It permits to "probe" the light-matter interaction directly *inside* the resonator, where light absorption takes place. Measuring the PTIR spectra of single cavities with varying patch size, the energy anticrossing signature of the strong coupling regime is reconstructed (Fig. 1b), with a good correlation with FTIR measurements over large arrays and with electromagnetic+thermal simulations. At last, by collecting PTIR maps of the patch surface at the resonance frequencies, the near-field coupling between the probe tip and the antenna can be imaged. The extracted profiles clearly show a single lobe for the (1,0) mode and a double lobe for the (2,0) mode (Fig. 1c), as qualitatively expected for the sinusoidal current distribution calculated from a simplified electromagnetic solution.

In conclusion we used PTIR nanoscopy to study strong light-matter coupling in single mid-IR resonators with intersubband transitions in semiconductor quantum wells. Both nanoimaging, nanospectroscopy and electromagnetic and thermal simulation results are reported.

References

[1] Todorov, Y., Andrews, A. M., Colombelli, R., De Liberato, S., Ciuti, C., Klang, P., ... & Sirtori, C. (2010). *Phys. Rev. lett*, *105*(19), 196402.
[2 Gillibert, R., Malerba, M., Spirito, D., Giliberti, V., Li, L., Davies, A. G., ... & Ortolani, M. (2020). *Appl. Phys. Lett*, *117*(10), 101104.

Revealing the Local Band Structures of 2D Materials by Near-Field Optical Imaging: Sharp WS_2/MoS_2 Heterojunction and Graded $W_xMo_{1-x}S_2$ Alloy

Po-Wen Tang[1], He-Chun Chou[1], Shiue-Yuan Shiau[2], Xin-Quan Zhang[3], Yi-Hsien Lee[3], and Chi Chen[1]*

1. Research Center for Applied Sciences, Academia Sinica, Taipei,115, Taiwan
2. Physics Division, National Center for Theoretical Sciences, Taipei, 106, Taiwan
3. Department of Materials Science and Engineering, National Tsing-Hua University, Hsinchu, 300, Taiwan

E-mail: chenchi@gate.sinica.edu.tw

Two-dimensional (2D) materials are promising for next-generation semiconductor devices and open the possibilities toward mesoscopic physics. With the development of various chemical vapor deposition (CVD) methods [1, 2], many artificial 2D semiconductors have been synthesized, which increases the chances of forming disrupted interfaces, non-periodic, or small-size systems (defects and grain boundaries). All such systems create local electronic band structures within a finite scale, which cannot be readily explained by the solid-state band theory nor be probed easily by confocal microscopes and macroscopic transport. Local probes, including structure (AFM), electronic states (STM or conductive AFM), and optical transition (SNOM), would be significant for mesoscopic, non-k-space physics.

Here, we investigated the abrupt heterojunction and the graded alloy between two transition metal dichalcogenides (TMD), which both involve with non-periodic band structures and require high spatial resolution. A homemade horizontal-type scanning near-field optical microscopy (SNOM) was developed to ensure high stability scanning over a long spectral acquisition time [3]. We employed near-field photoluminescence (NF-PL) imaging to study the atomically sharp 1D interfaces between the WS_2 and the MoS_2 (Fig. 1b). With an optical resolution of 68 nm, a 105 nm-wide region for quenched PL is confirmed with the NF-PL imaging, which is so far the best SNOM resolution in studying TMDs. Our NF-PL imaging resolved the narrowest quenching width and sharpest strain mapping due to the superior spatial resolution and stability of our home-built SNOM.

We further developed the near-field broadband absorption (or transmittance, NF-tr) imaging method to overcome the limitation of NF-PL in the case of low-quantum-yield materials. NF-tr technique provides the abbreviation-free and nanoscale-resolution imaging capability of the whole conduction bands over highly lateral inhomogeneity. We utilized the NF-tr microscopy to investigate the varying bandgap and the bowing factor of the single-layered $W_xMo_{1-x}S_2$ alloy. High-spatial-resolution spectral capability is essential for analyzing such compositional and location-dependent bandgap evolution. For bilayer $W_xMo_{1-x}S_2$ alloy (Fig. 1c), the energy contour maps present the bandgap evolution in the alloy and reveal the bilayer coupling between the top and bottom layers. We can conclude the alloy nature of the bottom layer, but the top layer is pure WS_2.

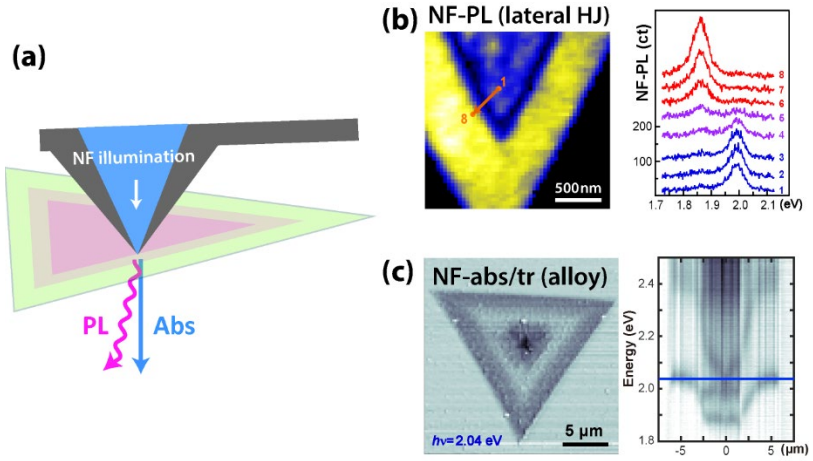

Fig. 1 Schematics of the near-field absorption/transmittance (NF-abs/tr) and near-field photoluminescence (NF-PL) measurements. (b) NF-tr spectroscopic imaging and band structure of the graded alloy. (c) NF-PL imaging and spectra of the lateral heterojunction.

References

(1) Zhang, X.-Q.; Lin, C.-H.; Tseng, Y.-W.; Huang, K.-H.; Lee, Y.-H. Synthesis of Lateral Heterostructures of Semiconducting Atomic Layers. *Nano Lett.* **2015**, *15* (1), 410–415.

(2) Chiu, K.-C.; Huang, K.-H.; Chen, C.-A.; Lai, Y.-Y.; Zhang, X.-Q.; Lin, E.-C.; Chuang, M.-H.; Wu J.-M.; Lee, Y.-H. Synthesis of In-Plane Artificial Lattices of Monolayer Multijunctions. Adv. Mater., 2018, 30, 1704796.

(3) Yu, J.-R.; Chou, H.-C.; Yang, C.-W.; Liao, W.-S.; Hwang, I.-S.; Chen, C. A Horizontal-Type Scanning Near-Field Optical Microscope with Torsional Mode Operation toward High-Resolution and Non-Destructive Imaging of Soft Materials. *Rev. Sci. Instrum.* **2020**, *91* (7), 073703.

Infrared correlation nanoscopy with unprecedented spectral coverage

Andreas J. Huber[1], **Tobias Gokus**[1], **Artem Danilov**[1], **Alexander A. Govyadinov**[1]

1. attocube systems AG (neaspec), Eglfinger Weg 2, 85540 Munich-Haar, Germany.

E-mail: andreas.huber@attocube.com

Nanoscale resolved imaging and spectroscopy using scattering-type Scanning Near-field Optical Microscopy (s-SNOM) or tapping AFM-IR (local detection of photothermal expansion) enables bypassing the ubiquitous diffraction limit of light and to achieve a wavelength-independent spatial resolution of <20 nm in the infrared (IR) frequency range [1,2]. Measurements have successfully demonstrated a wide range of analytical capabilities for e.g. nanoscale chemical mapping and material identification, conductivity profiling, determination of secondary structure of individual proteins and vector field mapping, making them a trusted tool for surface analysis in many branches of sciences and technology.

While s-SNOM and tapping AFM-IR provide nanoscale spatial resolution, applications are often limited by limited availability of illumination source, which prevents studies of low energy phonons, polaritons and molecular vibrations. This problem is partially circumvented by nanoscale Fourier transform infrared spectroscopy (nano-FTIR) – a potent s-SNOM technique – which can achieve large spectral coverage down to 320cm^{-1} (ca. 31µm wavelength) using ultrabroadband infrared radiation from synchrotrons [3]. However, nanoscale resolved imaging in the far-IR spectral range at wavelengths of e.g. >12 µm that provide rapid mapping of field or materials properties remains challenging due to lack of suitable table-top light sources with sufficiently small bandwidth (e.g. < 10 cm-^{1}).

Here we demonstrate s-SNOM and tapping AFM-IR imaging and spectroscopy based on a fully integrated and automated commercial OPO laser source covering the spectral range from 1.5 – 18.2µm (ca. 7100 – 540cm^{-1}) with narrow linewidth <4 cm^{-1} in the entire tuning range. Figure 1 shows a ca. 34nm thin hBN flake on a SiO substrate imaged by s-SNOM with interferometric detection in order to obtain nanoscale resolved amplitude and phase images of the propagating surface polariton mode. Clearly, the amplitude image at 810cm^{-1} reveals the characteristic fringe pattern at the edge of the flake stemming from propagating Surface Phonon-Polaritons (SPhP) launched by the AFM probing tip, which was not accessible previously.

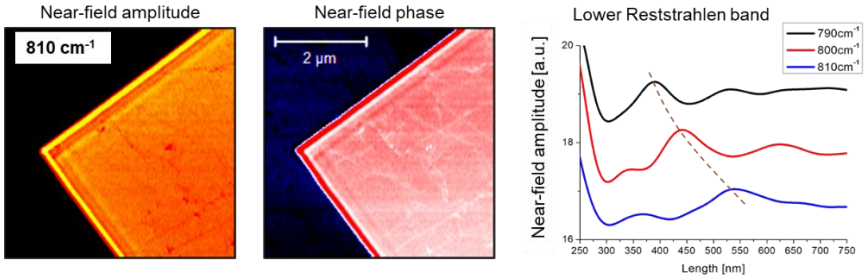

Fig. 1 hBN Surface Phonon-Polariton near-field imaging at the lower Reststrahlen band revealing characteristic fringes of propagating polaritons (amplitude left, phase center). Analysis of fringe spacing enables analysis of polariton dispersion as established for upper Reststrahlen band (right) [4].

Further, the methodology was successfully applied to selectively map the nanoscale spatial distribution of PVAC in a PS polymer matrix based on the 603cm^{-1} absorption line, allowing to study characteristic material heterogeneity and interfaces in the far-IR spectral range. Obtained results have been verified by correlative AFM-IR imaging with operating the laser at selected repetition rates. It is very important to mention that sweeping the laser frequency also allows to measure spectroscopic signatures of materials and other nanostructures with unprecedented spectral coverage, enabling studies of fundamental molecular resonances and quantum states in the long wavelength IR spectral range, which until now was not possible.

References

[1] F. Keilmann, R. Hillenbrand. 2004. *Philosophical Transactions of the Royal Society A: Mathematical, Physical and Engineering Sciences,* 362, 787–805.

[2] J. Jahng, A. O. Potma, E. S. Lee. *PNAS,* 116, 26359-26366.

[3] O. Khatib, H. A. Bechtel, M. C. Martin, M. B. Raschke, G. L. Carr. 2018. *ACS Phot.,* 5, 2773-2779.

[4] Q. Zhang, G. Hu, W. Ma, P. Li, A. Krasnok, R. Hillenbrand, A. Alú, C.W. Qiu. 2021. *Nature,* 597, 187-195.

High-fidelity nano-FTIR spectroscopy by on-pixel normalization of signal harmonics

Lars Mester[1,2], **Alexander A. Govyadinov**[2] und **Rainer Hillenbrand**[3,4]

1. CIC nanoGUNE BRTA, Tolosa Hiribidea 76, 20018 Donostia-San Sebastian, Spain
2. attocube systems AG, Eglfinger Weg 2, 85540 Munich-Haar, Germany
3. CIC nanoGUNE BRTA and Department of Electricity and Electronics, EHU/UPV, Donostia-San Sebastian 20018
4. IKERBASQUE, Basque Foundation for Science, 48011 Bilbao, Spain

E-mail: lars.mester@attocube.com

Scattering-type scanning near-field optical microscopy (s-SNOM) and Fourier transform infrared nanospectroscopy (nano-FTIR) are emerging tools for physical and chemical nanocharacterization of organic and inorganic composite materials. Being based on (*i*) diffraction-limited illumination of a scanning probe tip for nanofocusing of light and (*ii*) recording of the tip-scattered radiation, the efficient suppression of background scattering has been critical for their success. Here, we show that indirect tip illumination via far-field reflection and scattering at the sample can produce s-SNOM and nano-FTIR signals of materials that are not present at the tip position – despite full background suppression. Although these artefacts occur primarily on or near large sample structures, their understanding and recognition are of utmost importance to ensure correct interpretation of images and spectra. Detailed experimental and theoretical results show how such artefacts can be identified and eliminated by a simple signal normalization step, thus critically strengthening the analytical capabilities of s-SNOM and nano-FTIR spectroscopy.

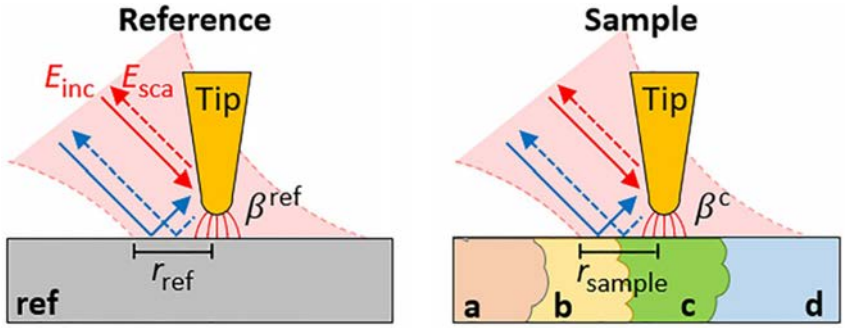

Fig. 1 Illustration of typical s-SNOM and nano-FTIR experiments. A metallized AFM tip near a known reference material (left) or unknown sample (right, generic sample composed of materials a, b, c, d) is illuminated by the electric field E_{inc} of a diffraction-limited infrared laser beam (red area). Near-field interaction between tip and sample modifies the tip-scattered light, E_{sca}, depending on the electrostatic reflection coefficient β_j of the material j below the tip apex. The tip is illuminated (and the tip-scattered light is detected) directly (red arrows) and indirectly via far-field reflection at the sample surface (blue arrows), depending on the far-field reflection coefficient r_j.

Near-field optical mapping of Dark excitons at room temperature based on Nano-imprinted pyramid probe

Junze Zhou[1], Edward Barnard[1], John Thomas[1], Elyse Barre[1], Archana Raja[1], Keiko Munechika[2], Adam Schwartzberg[1], Alexander Weber-Bargioni[1], Stefano Cabrini[1]

1. The Molecular Foundry, Lawrence Berkeley National Laboratory, Berkeley, CA 94720
2. HighRI Optics, Inc. Oakland, CA 94618.

E-mail: junzezhou@lbl.gov

Two-dimensional transition metal dichalcogenide (TMDCs) are direct bandgap materials with strong light-matter interactions in the visible light wavelength range. The light-induced exciton has binding energies as large as a few hundreds of meV at room temperature, which offers promising applications in optoelectronic devices[1, 2]. The presence of strong spin-orbit coupling in the energy bands of the monolayers results in the lowest energy exciton in WX_2 (X=S, Se) being spin-forbidden[3-6]. The theoretical study predicted the spin-dark excitonic emission is ~10^3 times lower than the bright one induced by this optical selection rule[7]. In addition, the optical access of dark exciton (X_D) is hampered by the out-of-plane polarization, which is difficult to excite and detect with the normally incident excitation photoluminescence measurement scheme[4]. Previously, several far-field approaches such as in-plane magnetic field[5], polarization-selective edge detection[4] have been proposed to observe the dark exciton. In near-field optics, Zhou et al.[8] used the silver thin film as the active substrate with an out-of-plane Purcell effect and coupled the X_D emission out at the edge of the substrate at cryogenic temperature. Park et al.[6] has applied a near-field probe to increase the radiative decay rate of the X_D at room temperature. So far, however, spatially resolved hyperspectral nano-PL mapping of X_D is still missing to explore how material heterogeneities impact the emission since reproducibly lifting the spin-forbidden selection rule with the scanning probe is challenging.

Here, we employ a reliable and mass-producible gap-mode geometry consisting of the ultra-flat Au thin film covered with a 2nm dielectric layer and a high-performance near-field probe to spectrally map out the X_D emission in 2d WSe_2. As shown in the right figure, we designed this gap-mode plasmonic configuration, based on the nano-imprinted scanning probe, for selectively enhancing the out-of-plane dipole emission, and enabling the near-field optical mapping of the dark exciton in a WSe_2 monolayer with the correlated topographic imaging. We demonstrated that the gap mode nanocavity could effectively enhance the out-of-plane X_D, which was observed at ~50meV blow the bright exciton (X_0), through a Purcell enhancement of more than 3 orders. The difference in spatial resolution of X_0 and X_D mappings indicate that the enhancement of X_D emission is localized within the nanogap. The correlation of gap-mode plasmonic enhancement and X_D was further confirmed by actively controlling the emission by changing the tip-sample distance. An optical resolution of ~30nm has been achieved through spatially resolved photoluminescence mapping, which is consistent with the curvature size of the nano-imprinted pyramid tip. This study demonstrates the outstanding correlated topographic and optical imaging performances of the nanoimprinted pyramid probe, providing a low-cost and high throughput technique in studying the optical properties of the new advanced quantum materials.

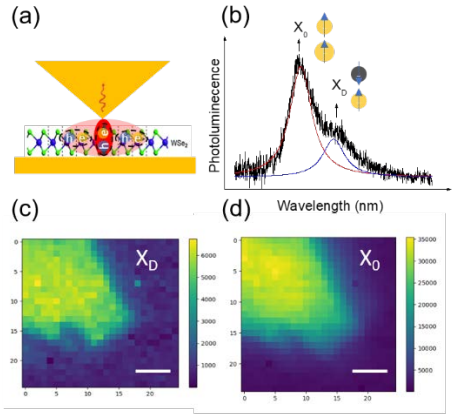

Fig. 1 Gap-mode plasmonic enhancement of PL emission based on the pyramid tip. (a) Schematic of the optical measurement configuration, which selectively enhanced the out-of-plane dipole emission. (b) PL spectrum of the WSe_2 monolayer collected through the gold pyramid tip shows both bright and dark excitonic emission features. The dark exciton (X_D) state is observed at ~50meV below the bright exciton (X_O). Integrated PL map ($2\times2\mu m^2$) of X_D (c) and X_O (d).

References

[1] A. Splendiani, L. Sun, Y. Zhang, T. Li, J. Kim, C.-Y. Chim, G. Galli, F. Wang, Emerging Photoluminescence in Monolayer MoS2, Nano Letters 10 (2010) 1271-1275.
[2] B. Radisavljevic, A. Radenovic, J. Brivio, V. Giacometti, A. Kis, Single-layer MoS2 transistors, Nature Nanotechnology 6 (2011) 147-150.
[3] R.J. Gelly, D. Renaud, X. Liao, B. Pingault, S. Bogdanovic, G. Scuri, K. Watanabe, T. Taniguchi, B. Urbaszek, H. Park, M. Loncar, Probing dark exciton navigation through a local strain landscape in a WSe2 monolayer, Nat Commun 13 (2022) 232.
[4] G. Wang, C. Robert, M.M. Glazov, F. Cadiz, E. Courtade, T. Amand, D. Lagarde, T. Taniguchi, K. Watanabe, B. Urbaszek, X. Marie, In-Plane Propagation of Light in Transition Metal Dichalcogenide Monolayers: Optical Selection Rules, Physical Review Letters 119 (2017) 047401.
[5] X.X. Zhang, T. Cao, Z. Lu, Y.C. Lin, F. Zhang, Y. Wang, Z. Li, J.C. Hone, J.A. Robinson, D. Smirnov, S.G. Louie, T.F. Heinz, Magnetic brightening and control of dark excitons in monolayer WSe2, Nat Nanotechnol 12 (2017) 883-888.
[6] K.-D. Park, T. Jiang, G. Clark, X. Xu, M.B. Raschke, Radiative control of dark excitons at room temperature by nano-optical antenna-tip Purcell effect, Nature Nanotechnology 13 (2018) 59-64.
[7] J.P. Echeverry, B. Urbaszek, T. Amand, X. Marie, I.C. Gerber, Splitting between bright and dark excitons in transition metal dichalcogenide monolayers, Physical Review B 93 (2016) 121107.
[8] Y. Zhou, G. Scuri, D.S. Wild, A.A. High, A. Dibos, L.A. Jauregui, C. Shu, K. De Greve, K. Pistunova, A.Y. Joe, T. Taniguchi, K. Watanabe, P. Kim, M.D. Lukin, H. Park, Probing dark excitons in atomically thin semiconductors via near-field coupling to surface plasmon polaritons, Nature Nanotechnology 12 (2017) 856-860.

Nano-optics of Epsilon Near Zero materials on metallic substrates

Flávio H. Feres[1,2,3], Ingrid Barcelos[1], Rafael A. Mayer[1,2], Raul de O. Freitas[1], Maximilian Obst[3], Tobias Nörenberg[3,4], Lukas M. Eng[3,4], Susanne C. Kehr[3], and Francisco C. B. Maia[1]

1. Institute of Physics "Gleb Wataghin", State University of Campinas (UNICAMP), Campinas, Sao Paulo, Brazil
2. Brazilian Synchrotron Light Laboratory (LNLS), Campinas, Sao Paulo, Brazil
3. Institute of Applied Physics, Technische Universität Dresden, 01062 Dresden, Germany
4. Dresden-Würzburg Cluster of Excellence-EXC 2147 (ct.qmat), 01062 Dresden, Germany

E-mail: flavio.feres@lnls.br

The manipulation of light at the nanometer length scale by means of photonic and quantum materials empowers the development of new optoelectronic devices and technologies [1]. In the kernel of light-matter interaction at nanometer length scales, high attention is directed towards low-dimensional materials, as are van der Waals (vdW) crystals [2,3], that have shown striking importance since providing strong light-matter interactions in the form of polariton waves. Some vdW materials such as the hyperbolic types, may intrinsically present anisotropic permittivities, where the real parts of the in-plane (ε_{xx} and ε_{yy}) and the out-of-plane (ε_{zz}) tensor components have opposite signs, i.e. $Re[\varepsilon_{xx,yy}] \cdot Re[\varepsilon_{zz}] < 0$, for certain excitation frequencies ω located between the transverse ω_{TO} and longitudinal ω_{LO} optical phonon branches [4]. Interesting phenomena arise whenever the excitation frequency meticulously approaches permittivity values near zero ($\varepsilon_{xx,yy,zz} \sim 0$) which exactly defines the epsilon near-zero (ENZ) zones. Within this scenario, intriguing optical effects are observed, including decoupling of electromagnetic fields [1], infinite impedance [5], slow-light [6], super transmission/reflection [7], and/or ultra-strong coupling to plasmonic structures [8]. Natural hyperbolic materials, such as hexagonal Boron Nitride (hBN) and alpha-Molybdenum Trioxide (α-MoO_3) possess this out-of-plane ENZ condition ($\varepsilon_{zz} \sim 0$), spanning from the mid-infrared (Mid-IR) to the terahertz (THz) regime.

In order to explore the influence of the ENZ condition of hyperbolic vdW crystals, we performed synchrotron infrared nano-spectroscopy (SINS) on α-MoO_3/Au samples. Fig 1a) shows the interference fringes (highlighted by the white dashed-line box) formed by standing waves between the tip and the crystal edge, propagating on the Au surface. These waves have both long wavelengths (up to $\lambda_p = 6\ \mu m$) and long propagation lengths (up to $L_p = 15\ \mu m$), due to the low light-confinement at the Au/air interface. Extracting the amplitude profiles for different frequencies, we observe that such waves only appear for frequencies near $1002\ cm^{-1}$, which exactly matches with the out-of-plane $\omega_{LO,zz}$ that corresponds to the ENZ ($\varepsilon_{zz} \sim 0$) mode. Note that the oscillation amplitude vanishes already for detuned frequencies $\omega_{LO,zz}$ of $\Delta\omega = 10\ cm^{-1}$ only, hence showing a highly narrow-band response. We interpret the phenomenon as the superposition of the far-field coming from the source reflected by the crystal and the surface plasmons polaritons (SPP) launched by the tip and reflected by the edges of the slab, where the reflection massively increases due to the ENZ, producing the interference pattern.

In conclusion, we understand that the out-of-plane hyperbolic crystal, concerning a general effect, can behave as a perfect mirror either for far-field or near-field optics at the ENZ frequencies, most specifically at $\omega_{LO,zz}$ frequencies.

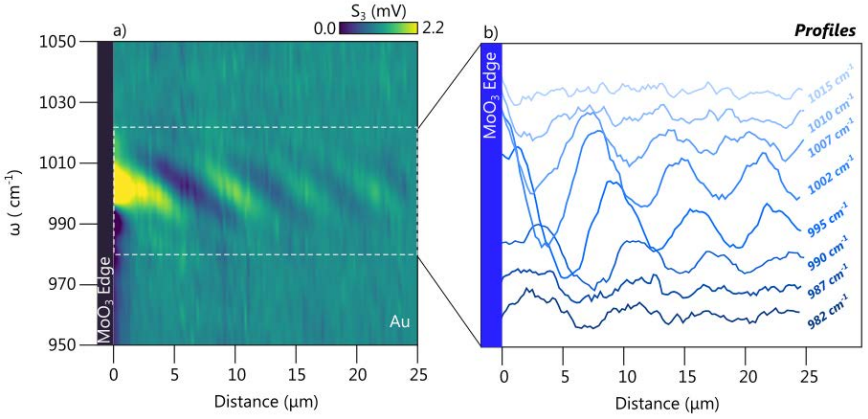

Fig. 1: a) Amplitude signal of the 3rd harmonic (S_3) of broadband spectral linescan performed by SINS on a 100-nm-thick α-MoO_3 crystal placed on a gold substrate; b) amplitude profiles extracted from the spectral linescan along the gold substrate, for different excitation frequencies ω.

References:

[1] Liberal, I. *et al*., 2017. *Nat. Phot.*, 11, 149-158.
[2] Low, T. *et al.* 2017. *Nat. Mat.*, 16, 182-194.
[3] Ferrari, L. *et al*., 2015. *Prog. Quantum Electron.* 16, 1-40.
[4] Narimanov, E. *et al*., 2015. *Nat. Photonics* 9, 214-216.
[5] Alù, A. *et al*., 2007. 75, 155410.
[6] Bello, F. *et al*., 2017. *Sci. Rep.* 7, 8702.
[7] Passler, N. C. *et al*., 2018. *Nano Lett.* 18, 4285-4292.
[8] Yoo, D. *et al*., *Nat. Photonics* 15, 125-130.

Focusing of In-plane Hyperbolic Polaritons in Van der Waals Crystals with Tailored Infrared Nanoantennas

Javier Martín-Sánchez[1], **Jiahua Duan**[1], **Javier Taboada-Gutiérrez**[1], **Gonzalo Álvarez-González**[1], **Kirill V. Voronin**[2], **Iván Prieto**[3], **Weiliang Ma**[4], **Qiaoliang Bao**[5], **Valentyn S. Volkov**[2], **Rainer Hillenbrand**[6], **Alexey Y. Nikitin**[7], **Pablo Alonso-González**[1]

1. University of Oviedo, Department of Physics c/ García Lorca, Oviedo, Spain
2. Moscow Institute of Physics and Technology, Russia
3. Institute of Science and Technology Austria IST, Am Campus 1, 3400 Klosterneuburg, Austria
4. Huazhong University of Science and Technology, Wuhan, China
5. Department of Materials Science and Engineering and ARC Centre of Excellence in Future Low-Energy Electronics Technologies (FLEET), Monash University, Clayton, Victoria 3800, Australia.
6. nanoGUNE BRTA and Department of Electricity and Electronics, UPV/EHU, Spain
7. Donostia International Physics Center (DIPC), Donostia-San Sebastián, Spain.

E-mail: javiermartin@uniovi.es

Polaritons -hybrid light-matter excitations- play a crucial role in fundamental and applied sciences, as they enable control of light on the nanoscale [1]. The recent emergence of low-loss van der Waals (vdW) materials opens the door to achieving anisotropic optical phenomena owing to their layered crystal structure, which leads to an intrinsic and strong out-of-plane (perpendicular to the layers) optical anisotropy. A prominent example is given by hyperbolic phonon polaritons (PhPs) -infrared light coupled to lattice vibrations in layered polar materials- in hexagonal boron nitride (h-BN) [2], which exhibit long lifetimes, ultra-slow propagation and hyper-lensing effects. Only recently, PhPs with in-plane hyperbolic dispersion, a key requirement for on-chip planar optical circuitry, have been demonstrated in natural slabs of α-phase molybdenum trioxide (α-MoO_3) [3-5] and vanadium pentaoxide (α-V_2O_5) [6].

In this work, we demonstrate focusing of infrared ray-like hyperbolic PhPs into deep subwavelength focal spots along the surface of α-MoO_3 crystals by using metal antennas with an optimized design. Specifically, field confinement is achieved in focal spots with a size of λp/4.5=λ0/50 (λp is the polariton wavelength and λ0 is the photon wavelength in free space). Moreover, the achievable focal distance in in-plane hyperbolic α-MoO_3 can be tuned to values well below the diffraction limit in in-plane isotropic materials, along with a better performance in terms of near field confinement and optical absorption. Our findings set the grounds for planar polaritonic technologies at the nanoscale [7].

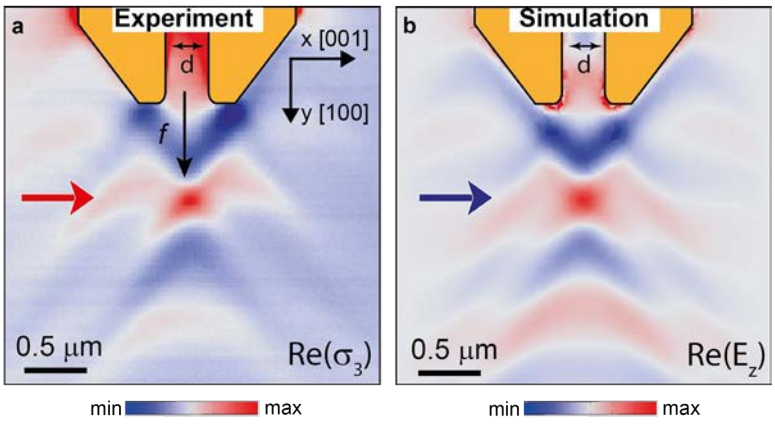

Fig. 1 Nanofocusing of phonon polaritons along the surface of a α-MoO_3 flake into deep-subwavelength focal spots ($\lambda_0/50$, being λ_0 the illuminating wavelength) using rod-like trapezoidal metal nanoantennas. The comparison between the experiment (a) and numerical simulations (b) are shown.

References

[1] Low, T., Chaves, A., Caldwell, J.D., Kumar, A., Fang, N.X., Avouris, P., Heinz, T.F., Guinea, F., Martin-Moreno, L., Koppens, F. 2017. *Nat. Mater.*, 16, 182.

[2] Dai,S., Fei, Z., Ma, Q., Rodin, A.S., Wagner, M., McLeod, A.S., Liu, M.K., Gannett, W., Regan, W., Watanabe, K, Taniguchi, T., Thiemens, M., Dominguez, G., Castro Neto, A.H., Zettl, A., Keilmann, F., Jarillo-Herrero, P., Fogler, M.M., Basov, D.N. 2014. *Science*, 343, 1125.

[3] Ma, W., Alonso-González, P., Li, S., Nikitin, A.Y., Yuan, J., Martín-Sánchez, J., Taboada-Gutiérrez, J., Amenabar, I., Li, P., Vélez, S., Tollan, C., Dai, Z., Zhang, Y., Sriram, S., Kalantar-Zadeh, K., Lee, S.T., Hillenbrand, R., Bao, Q. 2018. *Nature*, 562, 557.

[4] Duan, J., Capote-Robayna, N., Taboada-Gutierrez, J., Álvarez-Perez, G., Prieto, I., Martín-Sánchez, J., Nikitin, A.Y., Alonso-González, P. 2020. *Nano Lett.*, 20, 5323.

[5] Duan, J., Álvarez-Pérez, G., Voronin, K.V., Prieto, I., Taboada-Gutiérrez, J., Volkov, V.S., Martín-Sánchez, J., Nikitin, A.Y., Alonso-González, P. 2021. *Sci. Adv.*, 7, eabf2690

[6] Taboada-Gutiérrez, J., Álvarez-Pérez, G., Duan, J., Ma, W., Crowley, K., Prieto, I., Bylinkin, A., Autore, M., Volkova, H., Kimura, K., Kimura, T., Berger, M.-H., Li, S., Bao, Q., Gao, X.P.A., Errea, I., Nikitin, A.Y.,Hillenbrand, R., Martín-Sánchez, J., Alonso-González, P. 2020. *Nat. Mater.*, 19, 964.

[7] Martín-Sánchez, J., Duan, J., Taboada-Gutiérrez, J., Álvarez-Pérez, G., Voronin, K.V., Prieto, I., Ma, W., Bao, Q., Volkov, V.S., Hillenbrand, R., Nikitin, A.Y., Alonso-González, P. 2021. *Sci. Adv.*, 7, eabj012.

Observation of phonon polaritons in multilayer hexagonal boron nitride films grown by chemical vapor deposition

Calandrini Eugenio[1], Voronin Kirill[2], Balci Osman[3], Shinde Maruti Shinde[3], Sharma Subash[3], Barra Burillo Maria[1], Bylinkin Andrei[1, 2], Casanova Felix[1, 4], Hueso Arroyo Luis[1, 4], McAleese Clifford[5], Conran R. Ben[5], Wang Xiaochen[5], Kenneth Teo[5], Ferrari Andrea C.[3], Nikitin Alexey[2] and Hillenbrand Rainer[1, 4]

1. CIC nanoGUNE BRTA, Donostia - San Sebastián, Spain
2. Donostia International Physics Center (DIPC), Donostia - San Sebastián, Spain
3. Cambridge Graphene Centre, University of Cambridge, Cambridge CB3 0FA, United Kingdom
4. IKERBASQUE, Basque Foundation for Science, Bilbao, Spain
5. AIXTRON Ltd. Buckingway Business Park Anderson Rd, Swavesey, Cambridge CB24 4FQ, UK

Email: e.calandrini@nanogune.eu

Hexagonal boron nitride (hBN) is a heavily studied van der Waals (vdW) material that is able to support highly confined phonon polaritons (PhP) in the mid-infrared spectral range [1,2]. It inspired novel concepts in the field of nanoscale infrared imaging [3], field-enhanced infrared sensing [4] and vibrational strong coupling [5,6]. However, the typical approach for fabricating h-BN PhP devices relies on mechanical exfoliation of bulk crystals, viable only for proof-~~ }~~of-~~ }~~concept experiments due to its low yield. Although the interest in producing hBN and other vdW materials by other means is raising, PhPs on synthetized hBN were only reported on mono- and bilayers [7]. PhP nanoresonators and other devices based on such thin layers, however, may be unpractical for real-world applications due to very small extinction cross sections.

Here we present a combined scattering-type scanning near-field optical microscopy (s-SNOM) and far-field infrared spectroscopy study of wafer-scale hBN films of several nanometer thickness, which were grown by chemical vapor deposition (CVD) and transferred onto a Si/SiO_2 substrate.

We performed far-~~ }~~field reflection spectroscopy in order to extract the dielectric permittivity of the CVD grown hBN films and calculated the expected dispersion and lifetime of the PhPs. Interestingly, and in stark contrast to exfoliated hBN, s-SNOM imaging of the CVD grown material revealed random interference patterns all over the film (see Fig. 1) that we can attributed to ~~polariton~~PhP scattering at randomly distributed defects in the hBN layer. To analyze these patterns and determine the polariton dispersion and lifetime, we developed a theoretical ~~analysis~~ model and an experimental method ~~that result to confirm our predictions. I don't understand. Does not seem to make sense~~. Finally, we designed and etched hBN nanoribbons ~~displaying phonon polariton~~that exhibit transverse PhP resonances with quality factors ~50, which ~~is still competitive if compared to resonators made of natural hBN flakes~~are only a factor of about two smaller than that of PhP resoantors made of exfoliated hBN flakes [5]. Our study shows the potential of CVD-~~ }~~grown hBN layers to be used for large-~~ }~~scale fabrication of PhP based resonators and devices, e.g. for infrared sensing appliations.

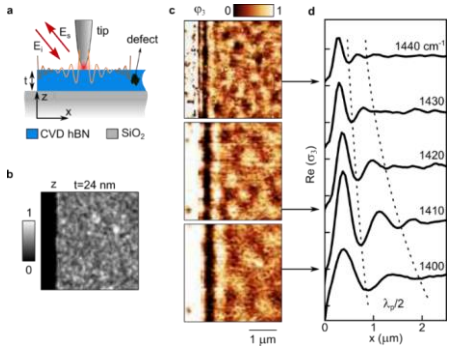

Fig. 1. a, Illustration of infrared s-SNOM imaging of PhPs in CVD-hBN. b. Topography image of a 24 nm thick CVD hBN film on SiO_2. c, Infrared s-SNOM phase images, revealing PhP interference fringes parallel to the hBN edge (analog to what is observed in s-SNOM images of exfoliated hBN flakes [6] but also random interference patterns far away from the edge (~~whidh~~which can be explained by polariton scattering at defects), d, Averaged s-SNOM profiles (showing the real part of the s-SNOM signal) extracted from panel d perpendicular to the hBN edge. The period of the signal oscillations ~~period~~ (corresponding to half of the polariton wavelength ~~insert $\lambda_p/2$~~) ~~is clearly shrinking with~~ decreases with increasing frequency, ~~indicating PhPs propagating.~~ revealing propagating PhPs.

References

[1] Basov, D N. 2016. *Science*, 354, 195.
[2] Dai S. 2014. *Science*, 343, 1125-1129.
[3] Li P. 2015. *Nat. Comm.*, 6, 1-9.
[4] Bareza N. 2022. *ACS Photonics*, 9, 34–42.

Formatted: Not Highlight

Formatted: Font: Symbol, 9 pt, Not Highlight

Formatted: Subscript, Not Highlight

Formatted: Font: Not Bold

Formatted: Font: Not Bold

Formatted: Indent: First line: 0 cm

[5] Autore M. 2018. *Light: Science & Applications*, 7, e17172.
[6] Bylinkin A. 2021. *Nat. Phot.*, 15, 197–202.
[7] Dai S. 2019. *Adv. Mater.*, 31, 1806603.

Anomalous coupling in hyperbolic medias

Lorenzo Orsini[1], **Hanan Herzig-Sheinfux**[1], **Iacopo Torre**[1], **Matteo Ceccanti**[1] **and Frank H. L. Koppens**[1]

1. ICFO, Av. Carl Friedrich Gauss 3, Castelldefels, Spain

E-mail: lorenzo.orsini@icfo.eu

In optics, photonic crystals are widely used to manipulate the dispersion of light and control its propagation. The possibility of creating metamaterials with optical properties exceeding the capabilities of natural materials has been investigated with great success in Silicon-based devices [1]. It has been shown that bringing this control to the nano-scale is extremely interesting to enhance light-matter interaction [2]. However, the Silicon platform has limited capabilities of confining light to subwavelength volumes. The alternative are polaritonic based metamaterial [3, 4], but the detrimental effect of absorption is still the main limiting factor. Recently, a new concept for confining light to the nanoscale using indirectly patterned hexagonal boron nitride (hBN) has been demonstrated [5]. In this material, multimodal nano-rays are the natural excitations, and the detrimental effect of absorption are neglected by multimodal effects (Fig. 1). Moreover, the coupling between these resonators is expected to inherit the multi-modal character of the resonance. This property can be used to produce very complex and rich metamaterials.

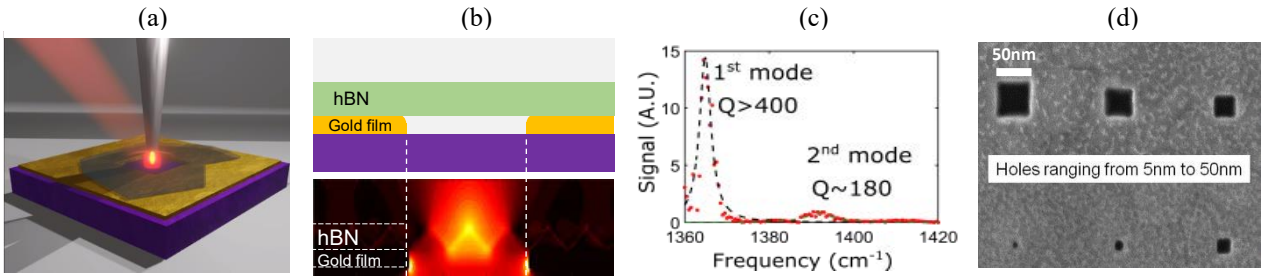

Fig. 1. **(a)** Illustration of the indirect patterned hyperbolic nano-cavity measured with sSNOM. **(b)** Top panel: illustration of the cross-section of the nano-cavity presented in (a). The hBN flake is suspended over a hole milled through a thin gold film. Bottom panel: color-plot showing the simulated electric field intensity $|E|^2$ at resonance of the structure illustrated above. The mode is well confined in the center of the cavity and the multi-modal character of this resonator is visible as nano-rays propagating inside the hBN slab at a fixed angle. **(c)** Quality factor measured with infrared near-field optical spectroscopy. **(d)** SEM image of the milled gold film showing the capability of reducing the size of a single nano-resonator down to $\sim 10nm$ x $10nm$.

Here, we study this multimodal coupling mechanism, experimentally and theoretically. An array of coupled resonators is designed to study how the coupling strength changes with respect to the separation distance (Fig. 2a). Using near-field microscopy we measure the resonance frequency of the coupled resonators. Notably, we observe a non-monotonic shift as the separation distance is increased (Fig. 2b). All in all, this is indicating the uniqueness of the coupling mechanism, since the most typical evanescent coupling would have produced a monotonically decreasing resonance shift. In conclusion, this peculiar coupling mechanism represents an alternative path to manipulate light on the extreme nanoscale, allowing the design of nanostructures with optical properties even richer than the traditional metamaterials. For example, photonic lattices hosting multimodal band-structures, enhanced next-nearest-neighbor coupling and second-order topological phases.

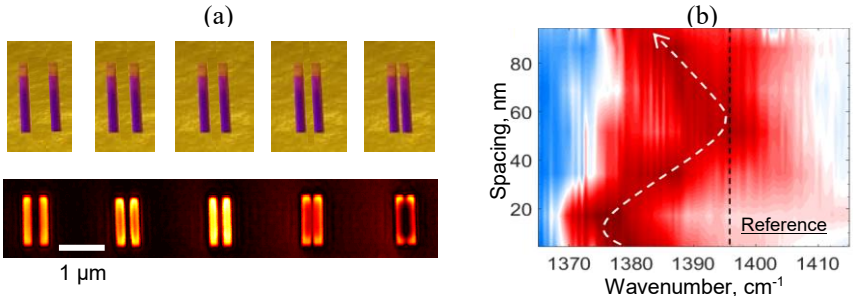

Fig. 2. **(a)** Top panel: illustration of the coupled resonators array of pairs having different separation distances. Bottom panel: near-field scan of the array shown above at 1380cm^{-1}. The different brightness along the array indicates that each pair has different resonance frequency. At this specific illumination frequency only the pair in the middle is resonating. **(b)** Color-map of the spectral response of many coupled resonators. Blue color indicates a weak response whereas the strong one is indicated in red. The black dashed line represents the resonance frequency of the isolated resonator used as a reference. The white dashed arrow is a guide to the eye, highlighting the non-monotonic resonance shifts.

References

[1] Staude, I., Schilling, J. 2017. *Nature Photon.*, 11, 274-284.
[2] Rider, M.S., Palmer, S.J., Pocock et al. 2019. *J. Appl. Phys.*, 125, 120901.
[3] Alfaro-Mozaz, F.J., Rodrigo, S.G., Alonso-González, P. et al. 2019. *Nat. Commun.*, 10, 42.
[4] Xiong, L., Forsythe, C., Jung, M. et al. 2019. *Nat. Commun.*, 10, 4780.
[5] Herzig-Sheinfux, H., Orsini, L., Jung, M. et al. 2022. *arXiv preprint, 08611v1*

Ordered and Disordered Porous Nanostructures for Passive Radiative Cooling

Azadeh Didari-Bader[1], **M. Pinar Mengüç**[2]

1. School of Basic Sciences, Hanbat National University, Yuseong-gu, Daejeon 34158, South Korea
2. Center for Energy, Environment and Economy, Ozyegin University, Cekmekoy, Istanbul 34794, Turkey
E-mail: azadeh@hanbat.ac.kr, pinar.menguc@ozyegin.edu.tr

The atmosphere's first transparency window (between 8-13 μm) coincides with the peak of the blackbody radiation spectrum for temperatures around 300 K. Within this window, nanophotonic systems can be designed to achieve radiative cooling even under direct sunlight. To realize this, designer systems should enhance thermal emission within the atmospheric transparency window and suppress it everywhere else outside of this window [1]. This allows the universe to act like a heat sink and lets the heat through the atmospheric window which greatly reduces the absorption of incoming atmospheric radiation. In order to design such selective emitters careful selection of materials and geometrical properties is important [2]. These designer nanophotonic systems could be used in radiative cooling applications such as in buildings, electronics and wearable technologies.

In this work, we present a systematic numerical analysis of various porous nanophotonic structures for radiative cooling applications. As shown in Fig. 1, ordered (left) and disordered (i.e., randomly distributed; right) are considered. Using a finite difference time domain (FDTD) method, we present the results for porous and mesoporous photonic systems made of materials such as TiO_2, SiO_2, ITO, W and phase change materials including VO_2 [3-4]. We analyze the impact of the frequency-dependent material properties and geometrical characteristics in order to identify the optimum selective emitters. We further perform optimization analysis on the geometrical characteristics such as radius of the pores, pore spacing and combined effects of pores of different sizes in these systems and identify the geometric properties that provide the optimum results for enhanced radiative cooling. The findings of this work can help the design of innovative structures to be used as selective thermal emitters.

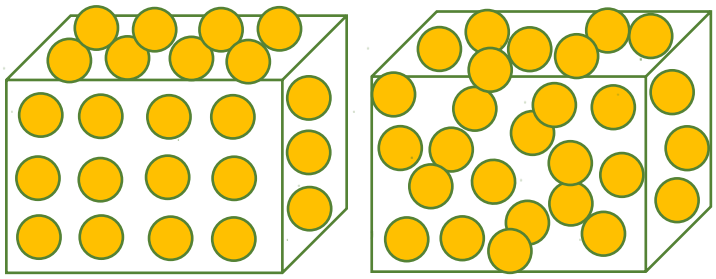

Fig. 1. Schematics of (left) ordered and (right) disordered nanophotonic systems considered for radiative cooling applications.

References

[1] Ono, M., Chen, K., Li, W., Fan, S. 2018. *Opt. Express* 26, A777-A787.
[2] Didari, A., Menguc, P. M. 2018. *Sci. Rep* 8 (1), 1-9.
[3] Wu, S. R., et al. 2018. *Sci. Rep* 8, 1-6.
[4] Gentle, A., et al. 2018. *Proc. SPIE* 10759, 107590L.

SQUEEZED STATES FROM PHOTONIC COOPER PAIRS

Sanker Timsina,[1,3] Filomeno S. de Aguiar Júnor,[2,3] Sahar Gholami Milani,[1,3] Alexandre Brolo,[2,3] and Rogério de Sousa[1,2]

[1]Department of Physics and Astronomy, University of Victoria, Victoria, British Columbia V8W 2Y2, Canada
[2]Department of Chemistry, University of Victoria, Victoria, British Columbia V8W 2Y2, Canada
[3]Centre for Advanced Materials and Related Technology,
University of Victoria, Victoria, British Columbia V8W 2Y2, Canada
Email: stimsina@uvic.ca

Raman scattering may generate entangled photon pairs when the same excitation created during a Stokes process is annihilated by another incoming photon. This correlated Stokes-antiStokes (SaS) process can also occur due to the exchange of virtual phonons, leading to a Hamiltonian that is identical to the one used in the Bardeen-Cooper-Schrieffer theory of superconductivity. Entangled photon pairs generated in this way are called photonic cooper pairs [1].

So far the SaS experiments are focused on coincidence measurements yielding large zero-time second order correlation $g^{(2)}(0)$, which proves that the photons are in a robust quantum state. While this demonstrates that the SaS process is a quantum phenomenon, it does not allow quantification of entanglement for quantum optics applications. Here we use the theory of photonic Cooper pairs to show that the ensemble of photonic Cooper pairs are actually in a multimode squeezed state. We calculate the degree of squeezing as a function of laser intensity and material properties, and discuss whether photonic Cooper pairs can be a useful resource in quantum sensing.

References

1. Saraiva, A., Júnior, F. S. D. A., De Melo E Souza, R., Pena, A. P., Monken, C. H., Santos, M. F., Jorio, A. (2017). *Physical Review Letters,* 119(19).

Electro-optical control of atomic bistability with graphene

Mikkel Have Eriksen[1], **Jakob E. Olsen**[1], **Christian Wolff**[1], **and Joel D. Cox**[1,2]
1. Center for Nano Optics, University of Southern Denmark, Campusvej 55, DK-5230 Odense M, Denmark
2. Danish Institute for Advanced Study, University of Southern Denmark, Campusvej 55, DK-5230 Odense M, Denmark
E-mail: cox@mci.sdu.dk

The intrinsically strong light-matter interactions available in graphene—the atomically-thin carbon layer—give rise to a broadband 2.3% light absorption that can be actively modulated by electrostatic gating; recent experiments confirm that the optoelectronic tunability of graphene can enable fast dynamical control of strong near-field interactions, leading to over 1000-fold decay enhancement of erbium emitters [1]. Highly-doped graphene also supports long-lived and actively-tunable plasmons that can dramatically enhance near-field coupling, but are limit to THz and IR parts of the electromagnetic spectrum, well-below the operational frequencies of robust quantum light sources [2,3]. Here we explore the optical bistability emerging from the self-interaction of an atom mediated by an extended sheet of highly-doped graphene, which we demonstrate can be harnessed to actively drive the atom into different quantum states (see Fig. 1). The strong electro-optical response of the graphene-atom hybrid system can be observed in the resonance fluorescence spectrum, which we predict to exhibit Mollow triplets and single Rayleigh peaks when electrically tuned through hysteresis loops. More specifically, we show that the Mollow triplets can be abruptly created or quenched in a manner reminiscent of a first-order phase transition in thermodynamics. Our findings motivate further experimental studies of driven atomic light emitters, while offering a prescription for active and *in situ* manipulation of quantum optical states in integrated nanophotonic platforms.

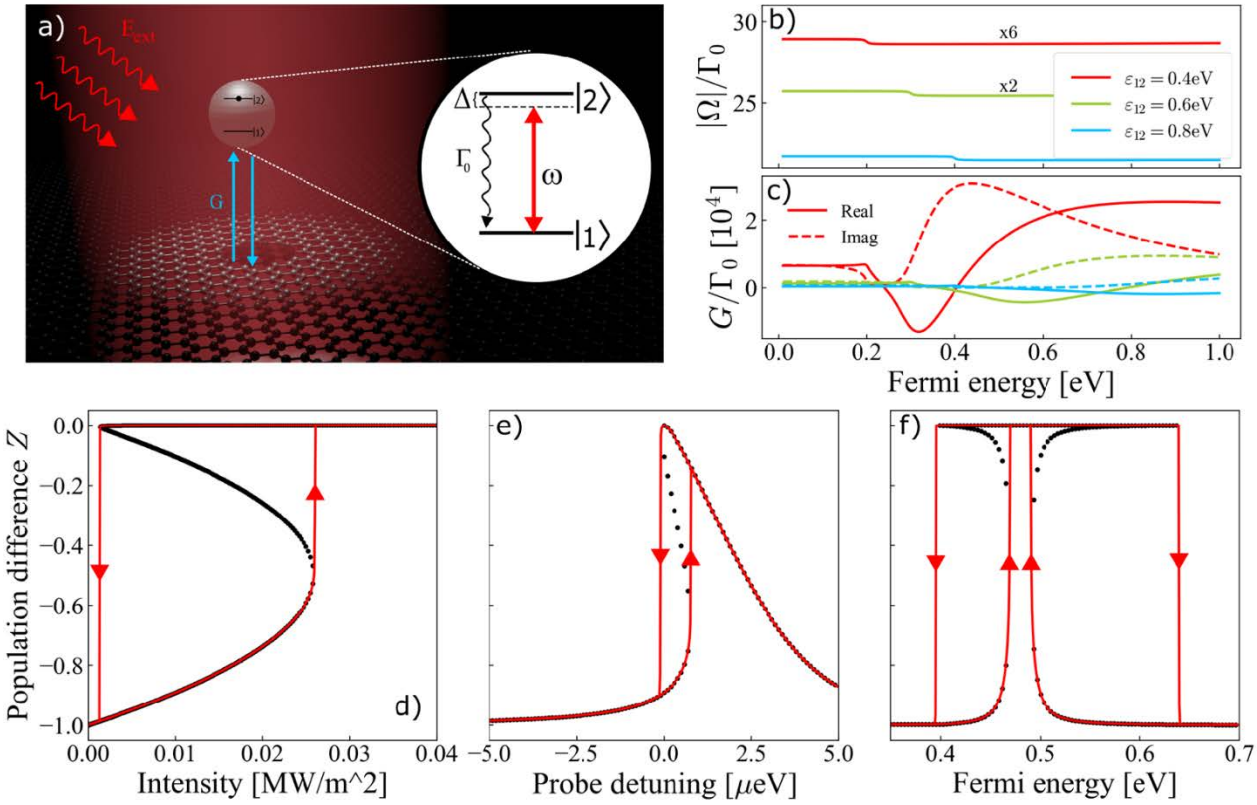

Fig. 1 Atom-field coupling of an optically-driven two-level atom interacting with a graphene sheet. (a) Schematic of the hybrid system comprised of a two-level atom above an extended graphene sheet driven by monochromatic light of frequency ω. (b) Atomic Rabi frequency Ω and (c) self-interaction G normalized to the intrinsic decay rate Γ_0 as functions of the graphene Fermi energy. Population difference in the two-level atom obtained by adiabatically sweeping the (d) light intensity, (e) frequency, and (f) graphene Fermi energy.

References

[1] Cano, D. et al. Fast electrical modulation of strong near-field interactions between erbium emitters and graphene. Nat. Commun. 2020, 11, 4094.
[2] Gonçalves, P. A. D., Stenger, N., Cox, J. D., Mortensen, N. A., and Xiao, S. Strong light-matter interactions enabled by polaritons in atomically-thin materials. Adv. Opt. Mater. 2020, 8, 1901473.
[3] Cox, J. D. and García de Abajo, F. J. Nonlinear atom-plasmon interactions enabled by nanostructured graphene. Phys. Rev. Lett. 2018, 121, 257403.

Study of correlated Stokes and anti-Stokes components in Surface-enhanced Raman Scattering

Filomeno Soares de Aguiar Junior, Sahar Gholami Milani, Sanker Timsina, Stanislav Konorov, Rogerio de Sousa, Alexandre Brolo.

1. University of Victoria - UVic

E-mail: filomenojunior@uvic.ca

The Raman scattering has two components: the Stokes (S) and anti-Stokes (aS). In the S process, one photon from the laser loses energy, creating one phonon in the sample, while in the aS process one photon gains energy by absorption of one phonon. When the same phonon created in the anti-Stokes process participates in the aS scattering, we have the correlated Stokes-anti-Stokes Raman Scattering, denominated SaS process, proposed by Klysko in 1976 [1]. The SaS is characterized by the scattering of a correlated S-aS photon pair, that was also observed out of resonance with the phonon energy in a process denominated virtual SaS. The virtual SaS is described by a formalism analogous to the BCS theory of superconductivity, putting these photons as photonic counterparts of Cooper pairs [2,3].

The SaS real and virtual processes were studied in many transparent materials, including diamond [4], water [5,2], and hydrocarbons [2]. The ability to generate correlated S-aS photon pair in Raman scattering has been explored in quantum optics and quantum information [6,7], used in the implementation of the quantum memory [8]. However, because of the low efficiency of SaS scattering, the observation of this phenomenon requires high laser power being achieved using pulsed lasers or electronic resonances [9]. Besides, the number of observed S-aS photon pairs is still low in comparison with other sources of correlated photon pairs, such as parametric conversion [4]. However, is expected to increase the S-aS intensity by increasing the quantum efficiency of conventional Raman scattering [3]. Thus, the Surface-enhanced Raman scattering (SERS) arises as a possible source of correlates SaS photon pair generation, once this technique can increase the Raman cross-sections values on the order of 10^8 or large [10]. In this work, we propose to investigate the SaS photon pair production from single-molecule, using SERS, looking for the enhanced intensity of the correlated Raman scattering.

References

[1] Klyshko, D. N. (1977). Correlation between the Stokes and anti-Stokes components in inelastic scattering of light. *Sov. J. Quantum Electron. Kvantovaya Elektron. (Moscow)*, *7*(4), 755–1341.

[2] Saraiva, A., Júnior, F. S. D. A., De Melo E Souza, R., Pena, A. P., Monken, C. H., Santos, M. F., Jorio, A. (2017). Photonic Counterparts of Cooper Pairs. Physical Review Letters, 119(19)

[3] Júnior, F. S. de A., Saraiva, A., Santos, M. F., Koiller, B., Souza, R. de M. e, Pena, A. P., Jorio, A. (2019). Stokes–anti-Stokes correlated photon properties akin to photonic Cooper pairs. *Physical Review B*, *99*(10), 100503.

[4]Kasperczyk, M., Jorio, A., Neu, E., Maletinsky, P., & Novotny, L. (2015). Stokes-anti-Stokes correlations in diamond. *Opt Lett*, *40*(10), 2393–2396.

[5]Kasperczyk, M., De Aguiar Júnior, F. S., Rabelo, C., Saraiva, A., Santos, M. F., Novotny, L., & Jorio, A. (2016). Temporal Quantum Correlations in Inelastic Light Scattering from Water. *Physical Review Letters*, *117*(24).

[6] Duan, L. M., Lukin, M. D., Cirac, J. I., & Zoller, P. (2001). Long-distance quantum communication with atomic ensembles and linear optics. *Nature*, *414*(6862), 413–418.

[7] Kuzmich, A., Bowen, W. P., Boozer, A. D., Boca, A., Chou, C. W., Duan, L.-M., & Kimble, H. J. (2003). Generation of nonclassical photon pairs for scalable quantum communication with atomic ensembles. *Nature*, *423*(6941), 731.

[8] Lee, K. C., Sussman, B. J., Sprague, M. R., Michelberger, P., Reim, K. F., Nunn, J., … Walmsley, I. a. (2011). Macroscopic non-classical states and terahertz quantum processing in room-temperature diamond. *Nature Photonics*, *6*(1), 41–44.

[9] Jorio, A., Kasperczyk, M., Clark, N., Neu, E., Maletinsky, P., Vijayaraghavan, A., & Novotny, L. (2014). Optical-phonon resonances with saddle-point excitons in twisted-Bilayer graphene. *Nano Letters*, *14*(10), 5687–5692.

[10] Langer, J., Jimenez de Aberasturi, D., Aizpurua, J., Alvarez-Puebla, R. A., Auguié, B., Baumberg, J. J., ... & Liz-Marzán, L. M. (2019). Present and future of surface-enhanced Raman scattering. *ACS nano*, *14*(1), 28-117.

Sensing Angular Momentum of Light using Cavity Optomechanical Coupled Oscillator System

Bishnupada Behera[1], **Hamidreza Kaviani**[1], **David Lake**[1], **Ghazal Hajisalem**[1], **Gustavo Luiz**[2] **and Paul Barclay**[1]

1. Institute for Quantum Science and Technology, University of Calgary,
2500 University Drive NW, Calgary, AB, T2N 1N4, Canada
2. nanoFAB Centre, University of Alberta, 116 St NW, Edmonton, AB, T6G 2V4, Canada
E-mail: bishnupada.behera@ucalgary.ca

It is well known that light has both linear as well as angular momentum. The circular polarization of light gives rise to spin angular momentum, and light's helical phase structure gives rise to orbital angular momentum, which is discrete and, in principle, unbounded [1]. This spatial structure of light enables access to a large state space which can be used to encode a large amount of information per photon. This characteristic feature of light has the potential for a wide range of applications in technologies such as in high bandwidth data transfer, optical tweezers, LIDAR, quantum communication, etc. Moreover, it is also known that light carrying spin or orbital angular momentum, upon interaction with any object can exert a mechanical torque on that object, although miniscule.

In a nanoscale structure consisting of an optical cavity, the strong interaction between light and mechanical oscillations enables very high precision optomechanical measurement [2] of force or torque. Here, as shown in Fig. 1, we present a novel experimental scheme involving an on-chip cavity optomechanical coupled oscillator system. This coupled oscillator system serves as a torque-sensing device with a sensitivity of $\tau_{min} \sim 10^{-22} - 10^{-19}$ Nm/√Hz for mechanical frequencies in the MHz-GHz regime. In this system, we have a nanomechanical torsional oscillator, i.e., a microdisk (md) suspended using two support beams (of length, *ls*). An intensity-modulated (red) laser beam carrying angular momentum upon incidence on the microdisk actuates/excites its in-plane torsional modes. The mechanical torsional motion of the microdisk is transduced to in-plane vibrational modes of an orthogonally connected suspended nanobeam (mb). This nanobeam (mb) along with another suspended nanobeam (rb) in parallel create an optomechanical two-beam photonic crystal 'zipper' cavity [3], to readout/transduce these hybridized torsional motion (excited in the mechanically coupled microdisk by light carrying angular momentum), onto the cavity laser field coupled into and out of the photonic crystal cavity using a tapered optical fiber.

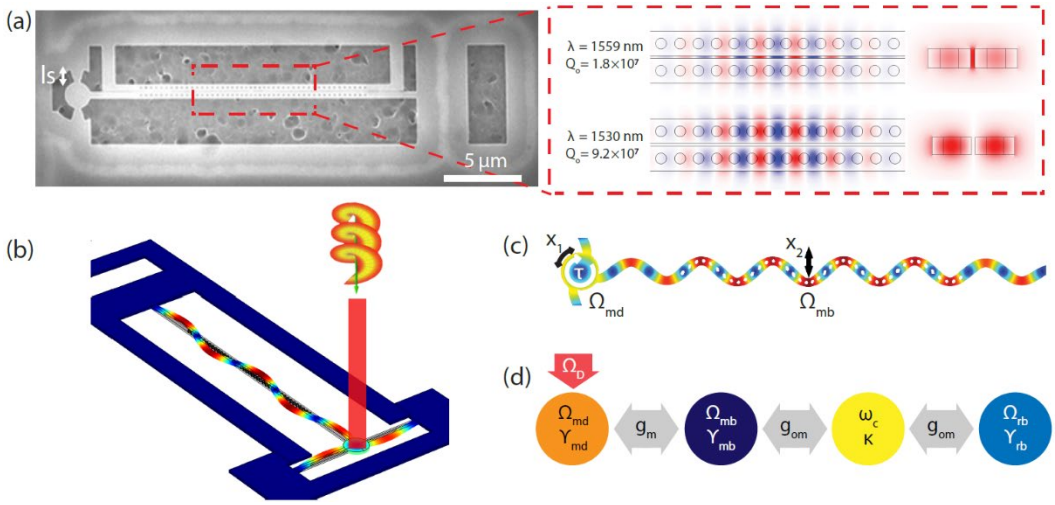

Fig. 1. (a) Scanning electron micrograph of the suspended microdisk-zipper cavity optomechanical device in Silicon, along with the optical field simulations of the two-beam photonic crystal 'zipper' cavity. (b) Schematic of actuation of the torsional motion. (c) Finite element simulation of an in-plane hybridized torsional mode of the device. (d) Coupled oscillator model for the torque-sensing device. [Ω_D: Intensity modulation frequency of the drive (red) laser carrying angular momentum, γ_{xx}: Dissipation rates of the mechanical oscillators/modes, κ: Decay rate of the optical cavity field, g_m: Mechanical coupling coefficient, g_{om}: Optomechanical coupling coefficient, Ω_{xx}: Mechanical mode(s) frequencies, ω_c: Optical cavity resonance frequency]

Our scheme/device provides a platform for interfacing free-space angular momentum carrying optical fields to on-chip nanophotonic components. This experiment not only opens the door for the study of interesting new dynamics of coupled nanomechanical torsional oscillators but also provides a foundation for ultra-sensitive torque/optical angular momentum measurement of single photon in the quantum regime.

References

[1] Allen, L., Beijersbergen, M.W., Spreeuw, R.J.C. and Woerdman, J.P., 1992. Orbital angular momentum of light and the transformation of Laguerre-Gaussian laser modes. Physical review A, 45(11), p.8185.
[2] Aspelmeyer, M., Kippenberg, T.J. and Marquardt, F., 2014. Cavity optomechanics. Reviews of Modern Physics, 86(4), p.1391.
[3] Eichenfield, M., Camacho, R., Chan, J., Vahala, K.J. and Painter, O., 2009. A picogram-and nanometre-scale photonic-crystal optomechanical cavity. nature, 459(7246), pp.550-555.

Circularly polarized light emission by incandescent metasurfaces

Anne Nguyen[1], **Anne-Lise Coutrot**[1], **Jean-Paul Hugonin**[1], **Enrique Garcia-Caurel**[2], **Benjamin Vest**[1], **Jean-Jacques Greffet**[1]

1. Université Paris-Saclay, Institut d'Optique Graduate School, CNRS, Laboratoire Charles Fabry, 91127 Palaiseau, FRANCE
2. LPICM, CNRS, Ecole polytechnique, Institut Polytechnique de Paris, 91127 Palaiseau FRANCE
E-mail: benjamin.vest@institutoptique.fr

Thermal emission is an intrinsically incoherent process, delivering broadband, isotropic and unpolarized radiation. Therefore, generation of a circularly polarized beam from an incandescent source generally requires the use of several components, such as filters and waveplates, in order to provide the adequate quarter-wave retardance within a limited range of frequencies. After these manipulation steps, a significant fraction of the beam energy is lost. Moreover, this approach limits the compactness of the whole light-emitting system. In our presentation, we report about the design, fabrication and characterization of a single ultrathin component, a thermal metasurface [1], designed to provide circularly polarized light in the mid-wave infrared domain.

The device consists of a three-layer structure: a back-reflecting gold mirror supporting a dielectric SiNx spacer whose top surface is paved with a subwavelength metallic grating. This grating is fabricated using thin platinum wires following a chiral pattern (see Fig. 1a)). The geometry of the system is optimized using a generalized Kirchhoff's law approach [2]. In other words, we design our system and estimate quantitatively its performances in emission using numerical calculations of its absorptivity. Our approach aims at maximizing both the overall efficiency of the device and its ability to generate light with a high degree of circular polarization.

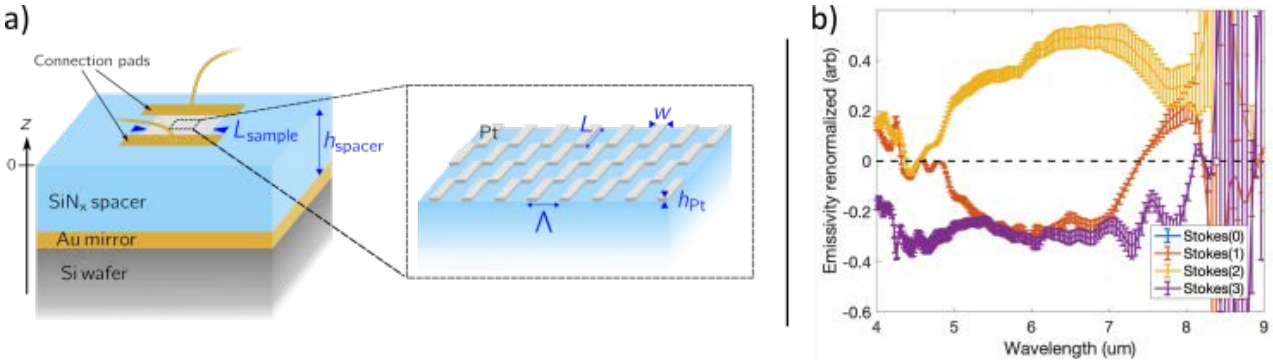

Fig. 1 a) Schematic of the device. **b)** Experimental determination of the Stokes parameters, based on emissivity measurements. Stokes(1) is proportional to the contrast in emissivity for polarization emitted at 0° and 90° (along and orthogonal to the grating period). Stokes(2) is proportional to the contrast in linear polarization emitted at 45° and -45° with respect to the same axis. Stokes(3) is proportional to the contrast between right-handed and left-handed circular polarization. This contrast is maximal aroud 4.5 um with negligible values for Stokes(1) and Stokes(2) on the same spectral domain. All values are normalized to the value of Stokes(0), the total emitted intensity.

The device operate in a Salisbury screen configuration. The thickness and permittivity of the spacer layer is chosen in order to maximize the absorption of an incoming light beam within the platinum grating [3]. Besides, the grating pattern and dimensions are chosen in order to make the grating a good chiral absorber: we maximize the contrast in absorption of the system when illuminated respectively by right-handed circularly polarized light (RCP) and left-handed circularly polarized light (LCP). The system is then turned into an incandescent metasurface by heating the top metallic grating by Joule effect. The contrast in absorptivity for LCP and RCP leads to a contrast in emissivity between LCP and RCP (see Fig 1.b)).

We report about the experimental performances of our devices. Our devices generate partially polarized light beams, with a near-zero degree of linear polarization (DLP) and a degree of circular polarization (DCP) ranging between 0.3 and 0.35 between 4.3 um and 4.8 um. The total degree of polarization increases up to 0.5 for longer wavelengths but is associated to more elliptical states of polarization.

Our system paves the way towards cheap and compact devices to generate infrared light with a decent DCP using only one single component, for applications in communication, sensing, security and counterfeiting.

References

[1] Overvig, A. C., Mann, S. A., & Alù, A. (2021). *Phys. Rev. X*, *11*(2), 021050. https://doi.org/10.1103/PhysRevX.11.021050
[2] Greffet, J.-J., Bouchon, P., Brucoli, G., & Marquier, F. (2018). Phys. Rev. X, 8(2), 021008. https://doi.org/10.1103/PhysRevX.8.02100
[3] Wojszvzyk, L., Nguyen, A., Coutrot, A. L., Zhang, C., Vest, B., & Greffet, J. J. (2021).. Nat. Comm., 12(1), 1–8. https://doi.org/10.1038/s41467-021-21752-w

Multipoles zoology made simple

Marco Riccardi, Andrei Kiselev, Karim Achouri and Olivier J.F. Martin

Nanophotonics and Metrology Laboratory, Swiss Federal Institute of Technology Lausanne (EPFL), Switzerland

E-mail: olivier.martin@epfl.ch

Most publications that study the response of nanophotonic structures – from an isolated nanostructure to the most complex metasurface – resort at one stage or the other to a multipoles analysis. Such analysis is very helpful to understand the spectral response of the system or the variations of its near-field distribution. The interplay between different multipoles leads to specific optical responses in the far-field, either very strong or very weak, depending on the multipoles that are interacting.

In spite of this ubiquity, multipoles can appear at first sight quite intricate since different multipoles families are needed to describe specific physical situations. Sometimes, a pair of electric and magnetic dipoles of vectorial nature that can be easily computed will suffice to obtain the response of the system. Often, higher order multipoles with a tensorial nature and concomitant complications are required. There are even situations that necessitate a seemingly completely different collection of so-called toroidal multipoles.

In this work, we clarify the multipoles zoology by reviewing three different approaches to calculate electromagnetic multipoles: the Cartesian primitive multipoles, the Cartesian irreducible multipoles and the spherical multipoles. We show that toroidal moments stem from the residuals that remain after expanding primitive multipoles into irreducible multipoles. We also study the influence of substrates and surfaces on the multipolar response of scattering systems and explain which multipoles family is the best suited to describe electromagnetic scattering by specific geometries and make a clear link with experiments.

Solar steam generation on scalable ultrathin thermoplasmonic TiN nanocavity arrays

Luca Mascaretti[1,#], **Andrea Schirato**[2,3,#], **Radek Zbořil**[1,4], **Štěpán Kment**[1,4], **Patrik Schmuki**[5], **Alessandro Alabastri**[6], **Alberto Naldoni**[1,7]

1. Regional Centre of Advanced Technologies and Materials, Faculty of Science, Palacký University, Šlechtitelů 27, 78371 Olomouc, Czech Republic
2. Department of Physics, Politecnico di Milano, Piazza Leonardo da Vinci 32, 20133 Milan, Italy
3. Istituto Italiano di Tecnologia, Via Morego 30, 16163 Genoa, Italy
4. Nanotechnology Centre, VŠB–Technical University of Ostrava, 17. listopadu 2172/15, 708 00 Ostrava-Poruba, Czech Republic
5. Department of Materials Science and Engineering, University of Erlangen-Nuremberg, Martensstrasse 7, D-91058 Erlangen, Germany
6. Department of Electrical and Computer Engineering, Rice University, 6100 Main Street, 77005 Houston, TX, United States
7. Institute of Fundamental and Frontier Sciences, University of Electronic Science and Technology of China, Chengdu 610054, China

# These authors contributed equally to this work

E-mail: luca.mascaretti@upol.cz

Solar-driven steam generation aims at exploiting the sunlight energy to vaporize water by means of a solar absorber. Among various materials, plasmonic-based absorbers can efficiently convert light to heat upon dissipation of plasmonic modes; furthermore, they can be fabricated in form of ordered quasi-two dimensional arrays, i.e., plasmonic metasurfaces, which exhibit broadband light absorption and promote a substantial heat generation thanks to collective photothermal effects.

In this work, we introduce a solar absorber based on a periodic array of titanium nitride (TiN) nanocavities. The absorber is enclosed within a custom-made PTFE cell that provides both thermal insulation as well as a water container in its top part, which is then illuminated by solar-simulated light (Fig. 1A). Unlike previously reported periodic structures, the present one features an ultrathin (~250 nm) nanocavity layer prepared by a scalable method consisting of electrochemical anodization of a Ti foil followed by nitridation in NH_3 atmosphere. In particular, the TiN nanocavities feature a self-ordered hexagonal array as a result of the anodization process (Fig. 1B) and, together with a Ti_2N underlayer, provide a broadband light absorption within ~300 nm from the sample surface. Numerical simulations reveal that the physical origin of such enhanced absorption is due to different resonant phenomena: pure cavity modes in the visible range (λ = 500 nm) and localized surface plasmon resonances at the cavity corners in the near-infrared (λ = 1700 nm). Water evaporation experiments performed with the custom PTFE cell under 1.4–14 Suns irradiation show a non-linear increase of the evaporation rate with light intensity, going from ~0.3-0.4 kg h^{-1} m^{-2} (comparable to water only and to the Ti plate substrate) up to ~14.9 kg h^{-1} m^{-2} for the TiN-based solar absorber (Fig. 1C), corresponding to ~76% efficiency. Numerical simulations further suggest the acceleration of the evaporation process in case of sub-µm thickness of both the TiN absorber and the water layer, paving the way for additional applications including nano-optofluidics and fast phase separation.

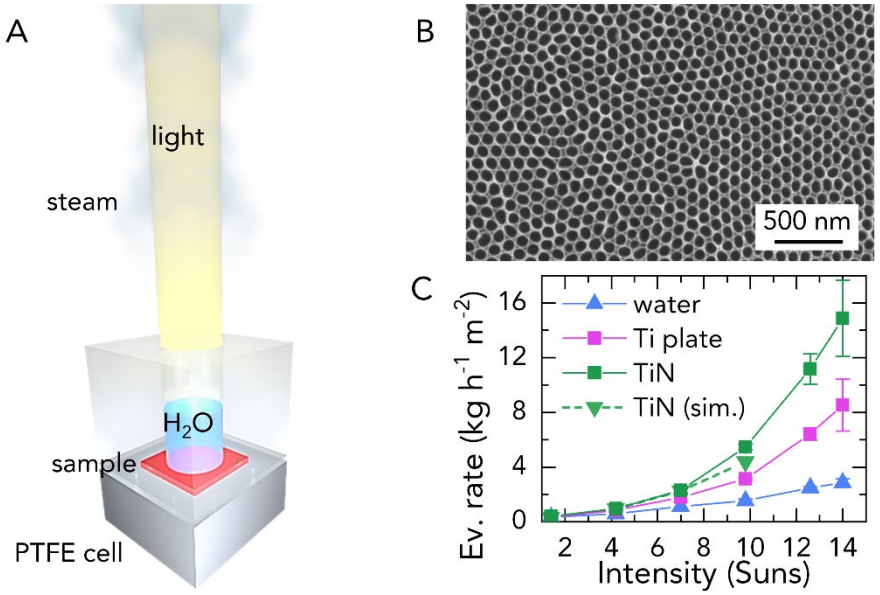

Fig. 1 (A) Schematic of water evaporation and steam generation by the TiN nanocavity sample under moderate light concentration in a custom-made PTFE cell. (B) Top-view scanning electron microscope image of the TiN nanocavities. (C) Evaporation rate under different light intensities (1 Sun = 1 kW m^{-2}) evaluated after 25 minutes for water only, a bare titanium substrate and the TiN nanocavities (the latter both experimentally and numerically). Reproduced from ref. [1]. Copyright 2021, Elsevier.

References

[1] Mascaretti L., Schirato A., Zbořil R., Kment Š., Schmuki P., Alabastri A., and Naldoni A. *Nano Energy* **2021**, *83*, 105828.

Influence of plasmonic substrate on the whispering-gallery modes in a π-conjugated polymer microsphere

Zhan-Hong Lin[1], Soh Kushida[2], Ching-Hang Chien[3], Jhih-Yuan Chen[4], Ankit Kumar Singh[1], Fan-Cheng Lin[3], Yohei Yamamoto[2], Yia-Chung Chang[3], and Jer-Shing Huang[1,3,4,5,6]

1. Leibniz Institute of Photonic Technology, Albert-Einstein Straße 9, 07745 Jena, Germany
2. Department of Materials Science and Tsukuba Research Center for Energy Materials Science (TREMS), Faculty of Pure and Applied Sciences, University of Tsukuba, 1-1-1 Tennodai, Tsukuba, Ibaraki 305-8573, Japan
3. Research Center for Applied Sciences, Academia Sinica, 128 Sec. 2, Academia Road, Nankang District, 11529 Taipei, Taiwan
4. Department of Chemistry, National Tsing Hua University, Hsinchu 30013, Taiwan
5. Abbe Center of Photonics, Friedrich-Schiller University Jena, Jena, Germany
6. Department of Electrophysics, National Chiao Tung University, 1001 University Road, 30010 Hsinchu, Taiwan

E-mail: jer-shing.huang@leibniz-ipht.de

We theoretically and experimentally study the influence of atomically flat gold substrate [1] on the whispering gallery modes (WGMs) in perfect fluorescent π-conjugated polymer microspheres [2] (Fig. 1a). Due to the large absorption coefficient of the polymer, excitation beam does not go into the sphere and the fluorescence only comes from the localized spot of laser focus. Therefore, we were able to select the emission position and thereby control the excitation of WGMs with different polarization states and orbitals. This allows us to study the effect of substrate on the WGMs. By analyzing excitation position dependent emission spectra, we observed different spectral shift and intensity change of the WGM spectrum, depending on the symmetry of the WGM and the material of the substrate. For intensity change, we observed clear symmetry selective damping of WGMs on gold substrate due to leakage into surface plasmons (Fig. 1b). For the spectral shift, we found peculiar and subtle spectral shift for the transverse-electric (TE) and transverse-magnetic (TM) WGMs depending on the mode symmetry and the substrate material (Fig. 1c).

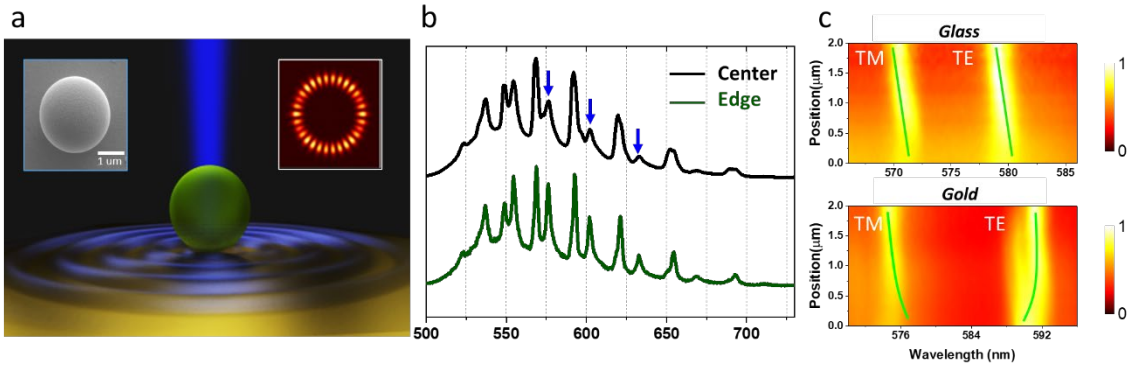

Fig. 1 (a) Illustration of the concept of this work. The left inset shows the SEM image of the sphere and the right one shows the simulated field distribution of the spheres in air. (b) Emission spectra of sphere from center (upper, black) and edge (bottom, green). The blue arrow indicates the peak leakage. (c) Spectral shift of TE and TM obtained from glass and gold substrate.

To understand the spectral shift, we constructed an analytical method based on full Green function within the Mie basis [4] and the Dyson equation including the substrate effect is solved numerically within the Mie basis. We found that the substrate effect produces a strong mixing of the resonant TE and TM modes that gives rise to significant mode shift and broadening. This work gains insight into the influence of gold substrate on the WGMs.

References

[1] J.-S. Huang et al., 2010 *Nat Commun.* **1**, 150.

[2] Adachi, T., Tong, L., Kuwabara, J., Kanbara, T., Saeki, A., Seki, S., Yamamoto, Y., 2013 *J. Am. Chem. Soc.* **135**, 870-876.

[3] Biagioni, P., Huang, J.-S., Hecht, B., 2012 *Rep. Prog. Phys.* 75, 024402.

[4] Mie, G., 1908 *Ann. Phys.* **25**, 377.

Giant mid-IR resonant coupling to molecular vibrations in plasmonic nanogaps

Rakesh Arul[1], **David Benjamin-Grys**[1], **Rohit Chikkaraddy**[1], **Niclas S Mueller**[1], **Ermanno Miele**[1], **Angelos Xomalis**[1], **and Jeremy Baumberg**[1]

1. NanoPhotonics Centre, Cavendish Laboratory, Department of Physics, University of Cambridge, United Kingdom

E-mail: ra554@cam.ac.uk

Nanomaterials capable of confining light across the visible to infrared (IR) spectrum are desirable for SERS and SEIRA spectroscopies, enhancement of nonlinear upconversion [1], and control of chemical reactions [2]. Here, we demonstrate how short-range-ordered Au nanoparticle multilayers (NPnML with n layers, Fig.1a), self-assembled by a precise sub-nm molecular spacer, support collective plasmon-polariton resonances in the IR region [3]. These resonances are continuously tunable beyond 11 μm (Fig.1c) by simply varying the nanoparticle size, number of layers, and by placing the NPnML on a mirror (Fig.1b). The collective plasmon-polariton mode is highly robust to nanoparticle vacancy disorder and is sustained by the consistent gap size defined by the cucurbit-5-uril (CB[5]) molecular spacer. We show these multilayers are easily fabricated and scalable, giving IR absorption enhancement for various molecular analytes.

The resulting molecule-plasmon system approaches the vibrational strong coupling regime [2], and displays giant Fano resonant dip strengths (Fig.1d) with SEIRA enhancement factors $\sim 10^6$, exceeding the enhancement of most state-of-the-art resonant plasmonic antennae fabricated through lithography [4]. Molecules within NPnML structures experience molecule-plasmon coupling strengths of $g \sim 100$ cm^{-1} and Purcell factors $\sim 10^6$ due to the compression of IR light into mode volumes $V_m \sim 10^{-8}\,\lambda^3$, resulting in strongly enhanced vibrational signatures. The small mode volume is a result of localization of the plasmon propagation due to disorder, and corresponds to 7 nanoparticle gaps, which is the average nanoparticle arrangement in a random close-packed structure.

The simplicity of self-assembly enables the creation of robust amorphous metasurfaces. Rather than being a burden, disorder is here a strength as it aids diffusion of molecules into the gaps. Structural disorder more efficiently couples light into the gaps between the multilayers and mirror, enabling real time SERS and SEIRA measurements of sub-picolitre sample volumes. We show how NPnML films allow sensing of various molecular analytes in a continuous flow geometry, and how the extraordinarily strong light-matter interaction within these structures supports collective light emission of quantum emitters.

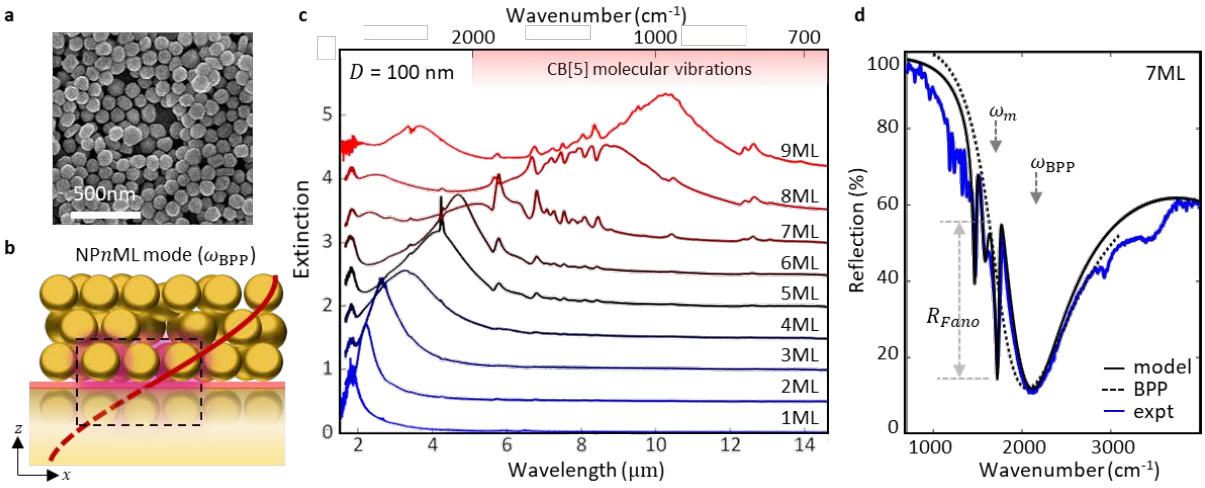

Fig. 1 Optical response of amorphous AuNP multilayers on gold (NPnML-on-mirror). (a) SEM of NP2ML film. (b) Mode from n = 3 layers of AuNP lattice-on-mirror. Red line depicts compression of the effective IR wavelength λ within the NPnML-on-mirror. (c) IR extinction spectrum of NPnML-on-mirror films for n = 1 to 9 with AuNP diameter D = 100 nm. Red shaded represents spectral region with molecular spacer cucurbit-5-uril (CB[5]) vibrational absorption peaks. (d) Fano lineshape of CB[5] vibration in coupled oscillator model (black line) with measured reflectance spectrum (blue line) of NP7ML-on-mirror films. Fano dip strength (R_{Fano}), molecular resonance (ω_m) and plasmon resonance (ω_{BPP}) labelled.

References

[1] Xomalis, A., Zheng, X., Chikkaraddy, R., Koczor-Benda, Z., Miele, E., Rosta, E., & Baumberg, J. J. *Science 374*, 1268 (2021)
[2] Garcia-Vidal, F. J., Ciuti, C., & Ebbesen, T. W. *Science*, *373*, 6551 (2021)
[3] Arul, R.; Benjamin-Grys, D.; Chikkaraddy R.; Mueller, N.S.; Xomalis, A.; & Baumberg, J.J. *submitted* (2022)
[4] Neubrech, F.; Huck, C.; Weber, K.; Pucci, A.; & Giessen, H.. *Chemical Reviews 117*, 5110 (2017)

A nanoscale plasmonic Su-Schrieffer-Heeger chain

Benedikt Schurr[1,5], **Philipp Grimm**[1], **Tobias Helbig**[2], **Tobias Hofmann**[2], **Lukas Wehmeier**[3], **Thorsten Feichtner**[1,4], **Monika Emmerling**[1], **Susanne C. Kehr**[3], **Lukas Eng**[3,5], **Ronny Thomale**[2,5] **and Bert Hecht**[1,5]

1. NanoOptics & Biophotonics Group, Experimental Physics 5, University of Würzburg, Am Hubland, 97074 Würzburg, Germany
2. Institute for Theoretical Physics and Astrophysics, University of Würzburg, Am Hubland, 97074 Würzburg, Germany
3. Institut für Angewandte Physik, Technische Universität Dresden, 01062 Dresden, Germany
4. Dipartimento di Fisica, Politecnico Milano, Piazza Leonardo da Vinci, 20133 Milano, Italy
5. Würzburg-Dresden Cluster of Excellence ct.qmat, University of Würzburg, Am Hubland, 97074 Würzburg, Germany

E-mail: benedikt.schurr@physik.uni-wuerzburg.de

The tight-binding Su-Schrieffer-Heeger (SSH) model describes 1D periodic chains of resonators with alternating coupling strengths. For certain configurations, topologically protected localized collective states occur at the edges, so called edge modes (Fig. 1 (a)). Such modes have recently been observed in low-frequency electric circuits [1].

Based on this concept, we propose a collinear plasmonic particle chain SSH-system with alternating gaps of a few nanometers in size. Simulations based on an efficient semi-analytical transfer matrix approach prove the existence of edge modes which manifest themselves by a deep reflection minimum within the plasmonic bandgap (Fig. 1 (b)) [2]. Furthermore, full FDTD simulations show the occurrence of edge modes for such geometries in real space. By focused He-ion beam milling, we are able to fabricate stable and nanometer precise plasmonic chains from single-crystalline gold micro-platelets (Fig. 1 (c)). Providing extraordinary control over particle size and coupling across the gaps, the frequency at which edge states occur can be fully controlled. Scattering scanning near-field optical microscopy (sSNOM) experiments indeed indicate the presence of topologically protected edge states (Fig. 1 (d)).

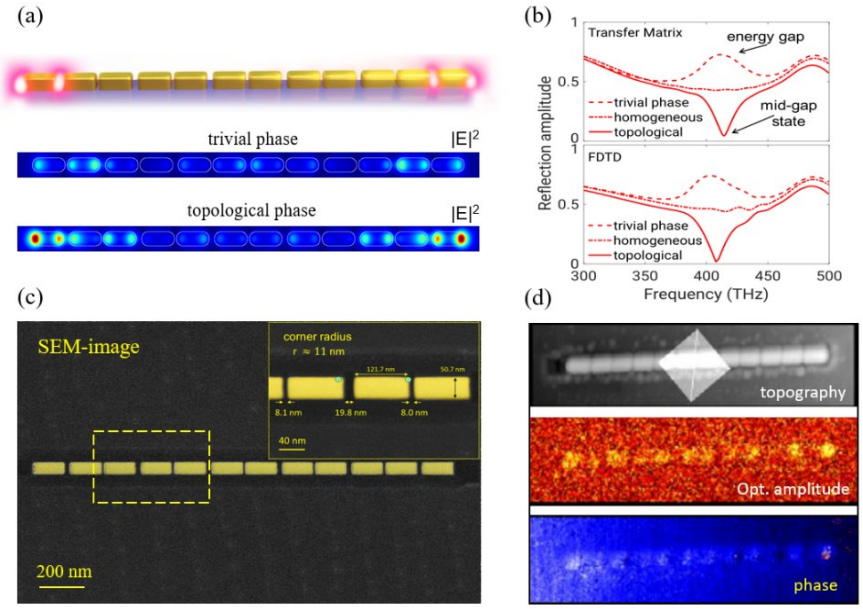

Fig. 1 (a) Artistic sketch of a nanoscale plasmonic Su-Schrieffer-Heeger (SSH) chain showing edge states. Below: Simulated electric field-distribution of trivial- and topological chain configuration. (b) Calculated and simulated reflection amplitude spectra of a chain system revealing a clear reflection minimum inside the energy gap for the topological phase. (c) Scanning electron microscope (SEM) image of a fabricated SSH-chain showing measured gap distances. (d) Experimental results of SNOM imaging showing topography (top), optical amplitude (middle) and optical phase (bottom).

References

[1] Lee, C.H., Imhof, S., Berger, C., Bayer, F., Brehm, J., Molenkamp, L.W., Kiessling, T., Thomale, R. 2018. *Commun Phys* **1**, 39
[2] Grimm P, Razinskas G, Huang J, Hecht B. 2021. *Nanophotonics* **10** (7). p. 1879-1887

Light-driven microdrones

Xiaofei Wu, Raphael Ehehalt, Gary Razinskas, Thorsten Feichtner, Jin Qin, and Bert Hecht

Nano-Optics and Biophotonics Group, Experimentelle Physik 5, Universität Würzburg, 97074 Würzburg, Germany
E-mail: xiaofei.wu@physik.uni-wuerzburg.de

Optical forces due to scattering or absorption of photons can be employed for remote manipulation of microscopic objects, especially for electrically and magnetically neutral ones, such as dielectric particles, biological cells, and atoms. However, until now, using light to control object motion in 2D/3D in all three/six degrees of freedom remains an unsolved challenge.

Here we present light-driven microdrones and demonstrate their systematic remote control in aqueous environment in 2D with all three independent degrees of freedom (forward-backward and right-left translations and clockwise-counterclockwise rotation), as seen in Fig. 1. The devices contain up to four specially designed plasmonic nanoantennas acting as thrust motors based on resonant directional light scattering, i.e., photon recoil. The nanomotors can be addressed individually by respective circular polarization components of unfocused light fields of two wavelengths, and therefore react independently of the in-plane orientation and position of the drone within the illumination. The microdrones can be steered in arbitrary paths by only adjusting the optical power for each motor (the power of each circular polarization component of each wavelength), which is very similar to the working principle of macroscopic quadcopters. The same concept can also be extended to 3D with all six degrees of freedom, without having to increase the number of light sources. Steering in all independent degrees of freedom would allow stabilization of position and orientation as well as the motion of the microdrones through automated feedback control. Owing to their unique properties, light-driven microdrones may serve as a novel experimental platform for many intriguing applications, such as transport and release of cargos, nanomanipulation, and local probing and sensing of nano and mesoscale objects.

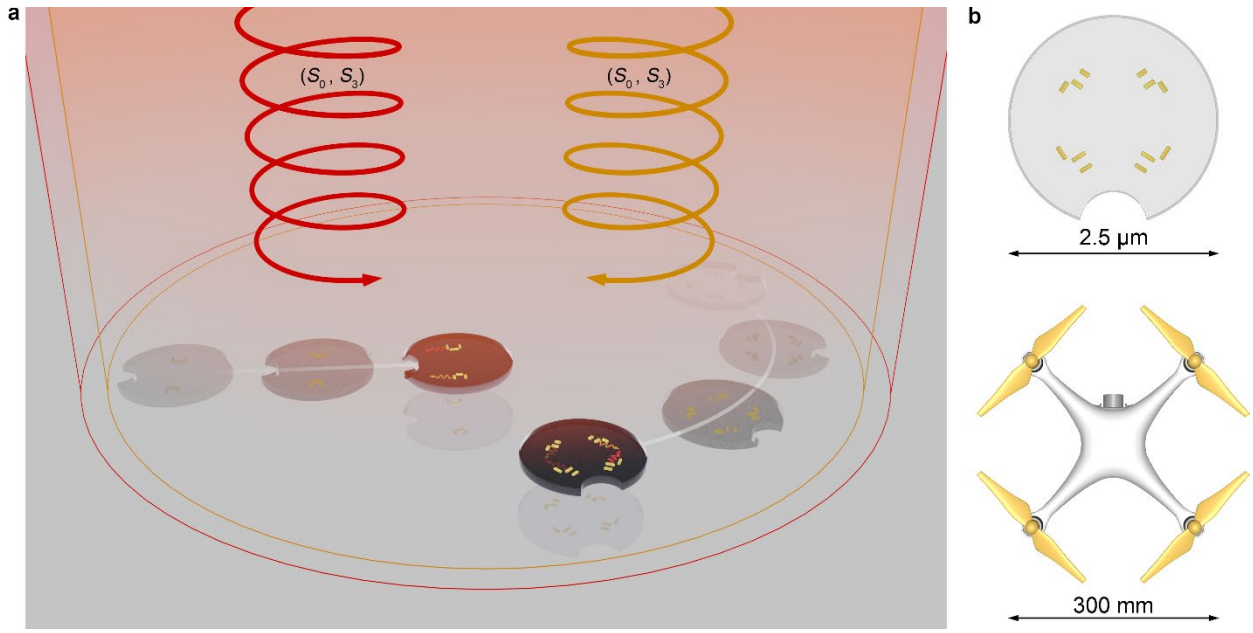

Fig. 1. Illustration of the setup and microdrone actuation concept. **a**, Two unfocused light beams of different wavelengths (orange, 830 nm and red, 980 nm) are used to steer two microdrones by adjusting the laser power and the polarization state, i.e., S_0 and S_3 of the Stokes parameters, of each beam. Gold nanoantennas integrated into the transparent body of the microdrone are resonantly excited by either of the two wavelengths and a certain circular polarization and then scatter light into defined lateral directions (indicated by the small wavy arrows), which leads to corresponding effective optical recoil forces. **b**, Top-view of the 4-motor microdrone (top) and comparison to a macroscopic quadcopter drone (bottom). Despite the tremendous difference in size, the motor configuration (two pairs of motors with opposite chirality) and steering principles (by only adjusting the power of each control channel) are very similar.

Reference

[1] Wu, X., Ehehalt, R., Razinskas, G., Feichtner, T., Qin, J., and Hecht, B. Light-driven microdrones. *Nat. Nanotech.* 2022, accepted.

Nonlinear Pumping of Molecular Vibrations in Plasmonic Nanocavities

Lukas A. Jakob[1], **William M. Deacon**[1], **Yuan Zhang**[2], **Elena Pavlenko**[1], **Rakesh Arul**[1], **Bart de Nijs**[1], **Niclas S. Müller**[1], **Tomas Neumann**[3], **Ruben Esteban**[3], **Javier Aizpurua**[3], **Jeremy J. Baumberg**[1]

1. NanoPhotonics Centre, Cavendish Laboratory, University of Cambridge, J J Thomson Avenue, Cambridge CB3 0HE, UK.

2. Henan Key Laboratory of Diamond Optoelectronic Materials and Devices, Ministry of Education, School of Physics and Microelectronics, Zhengzhou University, Zhengzhou 450052, China.

3. Center for Material Physics (CSIC - UPV/EHU and DIPC), Paseo Manuel de Lardizabal 5, Donostia-San Sebastian Gipuzkoa 20018 Spain.

E-mail: lj366@cam.ac.uk

When bound to metals, molecular vibrations play a key role in sensing, catalysis, molecular electronics, and beyond, but investigating their coherence and dynamics is difficult as pulsed experiments prove very challenging. Here we study vibrations of 1-100 molecules in a plasmonic nanocavity [1] (Fig.1a) when driven by ps-pulsed lasers out of the linear regime [2]. This unravels new nonlinear effects such as room-temperature vibrational pumping, giant optomechanical spring shifts [3], accelerated decay of vibrational energy [4], and SERS quantum correlations.

In plasmonic nanocavities, surface-enhanced Stokes scattering of a pulsed laser can significantly increase the phonon population above thermal equilibrium. This vibrational pumping leads to superlinear anti-Stokes scattering above a threshold laser power (Fig.1b). For different vibrational modes this threshold depends on their Raman cross section and energy. These molecular vibrations then interact with the optical cavity resonance via optomechanical coupling [5]. Due to Raman dipole image charges in the metal, this leads to a dramatic redshift of the vibrational energy by >100 cm^{-1} (optomechanical spring shift) and broadening of the Raman line at high peak laser powers [3].

To study the dynamics of these vibrations, we use time-resolved coherent anti-Stokes Raman scattering. Using a newly developed single-photon lockin-detection technique [6], we simultaneously record the decay of the vibrational population and the vibrational dephasing for each of >100 nanocavities. The vibrational decay is found to strongly accelerate at higher laser powers due to vibrational energy exchange with other modes [4]. Despite this accelerated decay, further experiments show that Stokes-induced anti-Stokes scattering exhibits strong quantum mechanical cross-frequency correlations (Fig.1c). These correlated Stokes/anti-Stokes photon pairs show non-classical breaking of the Cauchy-Schwarz inequality and can be used for applications in quantum computing and communication.

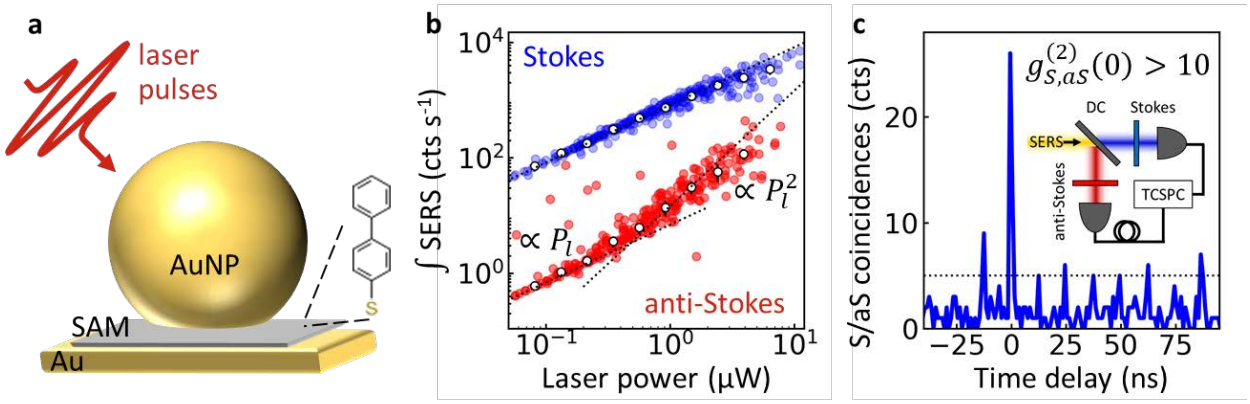

Fig. 1. (a) Monolayer of organic molecules in a plasmonic nanocavity under pulsed laser excitation. (b) Power dependence of Stokes and anti-Stokes scattering from nanocavity showing threshold of vibrational pumping. (c) Histogram of Stokes and anti-Stokes photon coincidences at single-photon detectors. Both photons are strongly correlated in a non-classical photon pair.

References

[1] Baumberg, J.J., Aizpurua, J., Mikkelsen, M.H., Smith, D.R. *Nat. Mater.*, 18, 668 (2019).
[2] Lombardi, A., Schmidt, M.K., Weller, L., Deacon, W.M., Benz, F., de Nijs, B., Aizpurua, J., Baumberg, J.J. *Phys. Rev. X*, 8, 011016 (2018).
[3] Jakob, L.A., Deacon, W.M., Baumberg, J.J. et al. *Submitted to Nat. Commun.* (2022).
[4] Deacon, W.M., Jakob, L.A., Baumberg, J.J. et al. *In preparation* (2022).
[5] Roelli, P., Galland, C., Piro, N., Kippenberg, T.J. *Nat. Nanotechnol.*, 11, 164 (2016).
[6] Jakob, L.A., Deacon, W.M., Hicks, O., Manyakin, I., Ojambati, O.S., Traxler, M., Baumberg, J.J. *Optica*, 8, 1646 (2021).

NFO16 Template

Strong Er^{3+} radiative emission enhancement by quasi-BIC modes coupling in all-dielectric slot nanoantenna arrays

Boris Kalinic[1], Tiziana Cesca[1], Ionut Gabriel Balasa[1], Andrea Jacassi[2], Riccardo Sapienza[2], Giovanni Mattei[1]

1. Department of Physics and Astronomy, University of Padova, Via Marzolo 8, I-35131 Padova, Italy
2. The Blackett Laboratory, Department of Physics, Imperial College London, London SW7 2BW, United Kingdom

E-mail: boris.kalinic@unipd.it

In the quest for new and increasingly efficient photon sources, the design of the photonic environment at the subwavelength scale is fundamental for controlling the emitter optical properties. It is well known, indeed, that the spontaneous emission rate of an emitter can be modified acting on its electric and magnetic local density of optical states (LDOS). Recently, all-dielectric high refractive index nanostructures have attracted increasing interest due to their unique optical properties (i.e., low absorption, optical magnetism, and multipolar responses) that can be exploited to enhance the optical properties of a nearby emitter without decreasing its quantum efficiency. However, the relatively modest Q-factors exhibited by electric and magnetic Mie resonances (Q~5-10) have limited the application of high-index nanoparticles in the enhancement of the LDOS. A possible way for obtaining orders of magnitude higher Q-factors in all-dielectric nanostructures is based on optical bound states in the continuum (BICs). Although true BIC can exist in structures that are infinitely extended at least in one direction, finite-size systems can support their analogue in the form of quasi-BICs, with the resonance quality factor that increases rapidly before reaching a maximum value limited by the finite-size effects. Despite the novelty of the field, quasi-BICs have already demonstrated their ability to outperform traditional photonic nanostructures for many photophysical processes usually limited either by losses or by low Q-factor resonances, such as second-and third-harmonic generation, light guiding, beam shaping, and sensing. Nonetheless, the realization of nanoantennas able to boost the emitter optical properties through an efficient coupling with q-BIC modes remains still an open issue [1].

In this framework, we propose a novel design for the all-dielectric nanoantennas supporting quasi-BICs, with an ultrathin silicon oxide layer doped with erbium ions placed inside slotted silicon nanopillars arranged in a square array (a sketch of the nanoantenna is shown in Fig. 1 (a)) [2,3]. Fig. 1(b) shows that a giant field intensity enhancement with an extremely narrow spectral width (Q~$2x10^5$) can be obtained at the resonance condition in the nanopillar region corresponding to the emitting layer. The reflectance has the asymmetric Fano-like line-shape of quasi-BIC modes where destructive interference of the scattered field outside the nanostructure brings to a strong enhancement of the near-field inside the nanoantenna. We demonstrate that by coupling the Er^{3+} radiative emission at about λ=1540 nm with quasi-BIC resonances, up to 3 orders of magnitude photoluminescence intensity increment and 2 orders of magnitude decay rate enhancement have been measured at room temperature (Fig. 1 (c)). Furthermore, acting on the nanoantenna aspect ratio, the emitter magnetic branching ratio can be tailored from 10% to 90%, keeping the quantum efficiency almost unitary. Finally, exploiting the reciprocity principle we were able also to design and control the emission directivity from the nanoslot, focusing more than 90% of the Er^{3+} emitted radiation at λ=1540 nm in a lobe normal to the sample surface with an angular width of Δθ<15. Hence, we have designed and realized CMOS compatible lossless nanoantennas able to boost the photon generation at telecom wavelength.

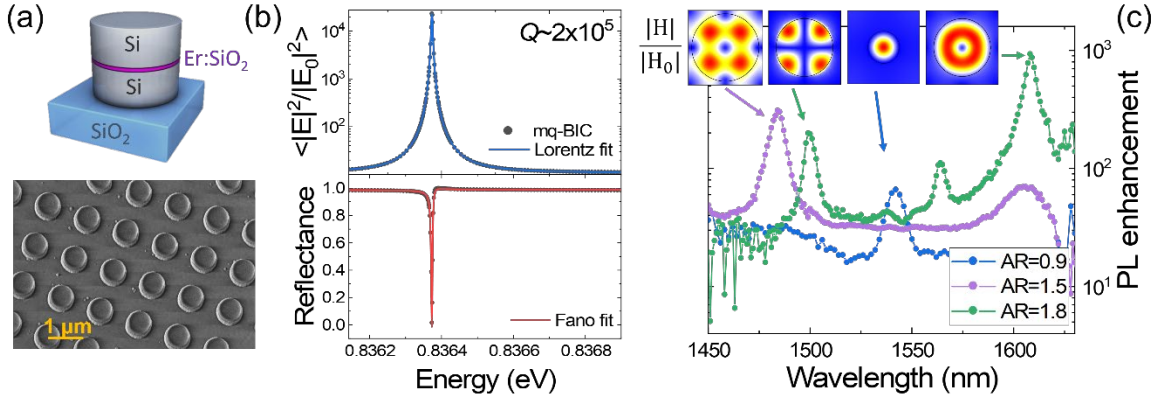

Fig. 1 (a) Sketch of the all-dielectric nanoantenna and a SEM image of the square array of slotted nanopillars. (b) The average electric field intensity enhancement in the SiO_2 slot and far-field reflectance for a plane wave impinging on the square array of slotted silicon nanoantennas with AR=1.5. (c) The Er^{3+} PL intensity enhancement in the λ=1450-1650 nm wavelength range for slotted nanopillars with increasing aspect ratio (AR=d/h). Upper panels report the magnetic field configuration ($|H|/|H_0|$) at quasi-BIC resonances.

References

[1] Kuznetsov, A. I., Miroshnichenko, A. E., Brongersma, M. L., Kivshar, Y. S., Luk'yanchuk, B. 2016. *Science*, 354, 6314.
[2] Mignuzzi, S., Vezzoli, S., Horsley, S. A., Barnes, W. L., Maier, S. A., Sapienza, R. 2019. *Nano Letters*, 19, 1613–1617.
[3] Kalinic, B., Cesca, T., Mignuzzi, S., Jacassi, A., Balasa, I. G., Maier, S. A., Sapienza, R., Mattei, G. 2020. *Phys. Rev. Appl.*, 14, 14086.

Invited: Plasmonic hot carriers and their application in catalysis

Pierre Berini
School of EECS, University of Ottawa, 25 Templeton St, Ottawa, Canada, K1N 6N5
Department of Physics, University of Ottawa, Ottawa, Canada
E-mail: berini@eecs.uottawa.ca

Plasmonics has evolved explosively over the last two decades to become a hallmark of nanophotonics. Applications are abundant, including, *e.g.*, biosensors, optoelectronics, devices for telecom, spectroscopy, decorative texturing, anticounterfeit markings, and catalysis. A recent and exciting direction of investigation concerns the ability of surface plasmon polaritons (SPPs) to generate energetic carriers in metals, and the subsequent harvesting of such carriers to alter fundamental processes and open new applications [1].

SPPs are TM-polarised surface waves guided by a metal-dielectric interface at optical wavelengths. They are supported as propagating modes on metal waveguides or as resonant modes on metal nanoparticles, nanoantennas or gratings. They are strongly localized to the metal surface, and under certain conditions are strongly absorbed therein, leading to the effective creation of energetic carriers - "hot electrons" and/or "hot holes" - also localized along the surface. These energetic carriers can be harvested and used for a broad range of applications, *e.g.*, to enhance the performance of optoelectronic and photovoltaic devices, or to open new reaction pathways in chemistry. Recent and ongoing progress along these threads will be discussed, including the reduction of CO_2 to solid light-emitting carbon dots [2], and the opening of new redox channels in electrochemistry [3].

The left panel of Fig. 1 shows a series of SERS spectra evolving over time as a Ag grating under SPP excitation is excited by green light (532 nm) under CO_2 exposure in a gas flow cell [2]. The spectra indicate growth of photoluminescent graphitic carbon on the surface, taking the form of spherical deposits that are visible under helium microscope (Fig. 1, middle panel). The observed luminescence consists of yellow light and persists as long as CO_2 exposure is maintained (Fig. 1, bottom left panel).

The right panel of Fig. 1 shows cyclic voltammograms obtained under SPP excitation of the working electrode, shaped as a Au stripe waveguide, as a function of incident optical power (λ_0 ~1350 nm) [3]. Processes involving energetic holes are separated from processes involving energetic electrons by investigating oxidation and reduction reactions separately. Redox current densities increase by 10× under SPP excitation. The oxidation, reduction and equilibrium potentials decrease by as much as 2× and split in correlation with the photon energy beyond a clear threshold with SPP power. Electrochemical impedance spectroscopy reveals a drop of almost 2× in charge transfer resistance under SPP excitation.

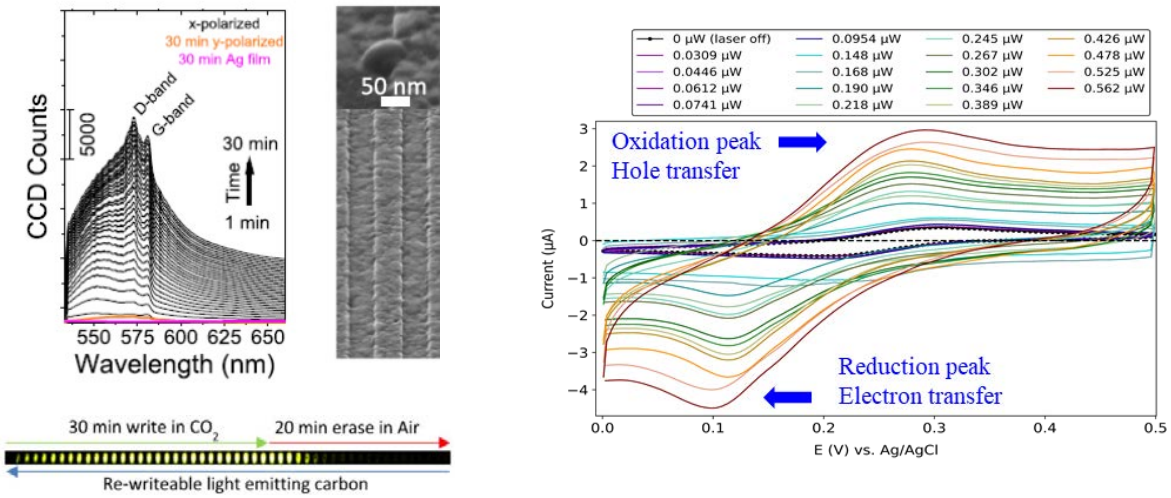

Fig. 1. Left panel: SERS spectra evolving over time showing the growth of solid carbon deposits in CO_2. Middle panel: helium ion microscope image of carbon nanodots on a Ag grating. Left bottom panel: increase and decrease of yellow light emission as carbon nanodots form then disappear. Right panel: cyclic voltammogram of $K_4[Fe(CN)_6] \leftrightarrow K_3[Fe(CN)_6] + e^-$ in KNO_3 electrolyte with increasing SPP power (legend). Left panels: [2], right panels: [3].

References

[1] Brongersma, M. L., Halas, N. J., Nordlander, P., "Plasmon-induced hot carrier science and technology," *Nature Nanotechnol.* **10**, 25 (2015)
[2] Walia, J., Rashid, S., Killaire, G., Weck, A., Berini, P., "Reconfigurable carbon quantum emitters from CO_2 gas reduced via surface plasmons," *Optica* **8**, 708 (2021)
[3] Hirbodvash, Z., Krupin, O., Northfield, H., Olivieri, A., Baranova, E. A., Berini, P., "Infrared surface plasmons on a Au waveguide electrode open new redox channels associated with the transfer of energetic carriers," *Science Advances*, in press

Hot electrons in metal nanostructures – “reality” or “fake news”?

Yonatan Sivan[1], Ieng Wai Un[1], Joshua Baraban[2], Yonatan Dubi[2]
1. School of Electrical Engineering, Ben-Gurion University of the Negev, Be’er-Sheva 8410501 Israel
2. Department of Chemistry, Ben-Gurion University of the Negev, Be’er-Sheva 8410501 Israel
E-mail: jdubi@bgu.ac.il

We present a self-consistent theory of the steady-state electron distribution in metals under continuous-wave illumination which treats, for the first time, both thermal and non-thermal effects on the same footing [1]. We show the number of non-thermal electrons (i.e., the deviation from thermal Fermi-Dirac equilibrium) is very small, so that the power that ends up generating these non-thermal electrons is many orders of magnitude smaller than the amount of power that leads to regular heating. We will review briefly an experimental confirmation of our prediction and its relevance to plasmonic nanostructures of various sizes and shapes.

Using this theory, we re-examine the exciting claims on the possibility to enhance chemical reactions with these non-thermal electrons, claims which have been pushed forward by various experimental groups, and published (with essentially no theoretical confirmation) in top journals. We identify a series of rather astounding errors in the temperature measurements in some of the most famous papers on the topic which led their authors to under-estimate regular heating effects. As an alternative, we show that a very simple 19th century theory, based on just simple heating, can explain the published experimental data with excellent accuracy [2,3].

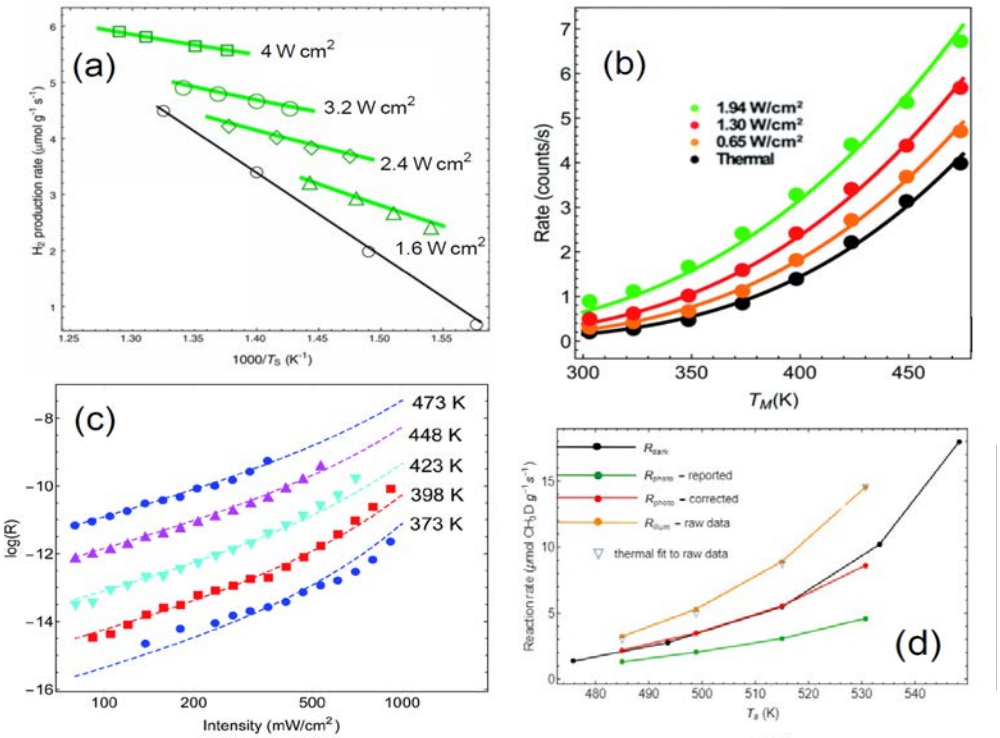

Fig. 1 Experimental data (symbols) and fits using the classical Arrhenius theory (lines), showing remarkable agreement. Data collected from high-impact papers that claimed (incorrectly) for dominance of non-thermal effects.

References

[1] Y. Dubi, Y. Sivan, “Hot electrons in metallic nanostructures - nonthermal carriers or heating?,” Light: Science & Applications 8, 89 (2019). Y. Sivan, I.W. Un, Y. Dubi, “Assistance of plasmonic nanostructures to photocatalysis – just a regular heat source,” Faraday Discussionss **214**, 215 – 233 (2019).

[2].Y. Sivan, J. Baraban, I.W. Un, Y. Dubi, “Comment on “Quantifying hot carrier and thermal contributions in plasmonic photocatalysis””. Science 364 (6439), eaaw9367 (2019). Dubi, I.W. Un, Y. Sivan, “Thermal effects – an alternative mechanism for plasmon-assisted photocatalysis”. Chemical Science 11, 5017-5027 (2020). Y. Sivan, J. Baraban, Y. Dubi, “Experimental practices required to isolate thermal effects in plasmonic photo-catalysis – lessons from recent experiments”. OSA Continuum 3, 483-497 (2020). Y. Dubi, I.E. Un, J. Baraban, , Y. Sivan, “Matters Arising in “Plasmon-driven carbon–fluorine (C(sp3)–F) bond activation with mechanistic insights into hot-carrier-mediated pathways”. Nature Catalysis, accepted.

[3] Y. Dubi, I.W. Un, J. Baraban & Y. Sivan, “Distinguishing thermal from non-thermal contributions toplasmonic hydrodefluorination”, Nature Catalysis (2022, accepted).

Theory of metallic nanostructures photoluminescence under continuous pumping

Aurelian Loirette--Pelous[1], **Mondher Besbes**[1], **Jean-Jacques Greffet**[1]

1. Université Paris-Saclay, Institut d'Optique Graduate School, CNRS, Laboratoire Charles Fabry,91127 Palaiseau, France

E-mail: aurelian.loirette-pelous@institutoptique.fr

In the past decades, metallic nanostructures have received a great attention due to their ability to confine electric fields in the nanoscale. For long, it has been remarked that such structures emit light over a broad spectral range [1], akin to fluorescence of molecules, both under pulsed and continuous pumping. While under pulsed pumping, electrons can reach very high temperatures leading to blackbody emission in the visible range, this emission turns negligible under continuous pumping. Instead, intraband recombination of high energy ("hot") electrons induced by pumping has been pointed out, and the corresponding non-equilibrium electron distribution calculated [2]. However, quantitative predictions of the emitted light still lack from a unified formalism considering the modal landscape in which the emission occurs.

Here, we show that the spectrum, the angular dependence and polarization of the photoluminescence from arbitrary metallic nanostructures can be calculated easily using a generalization of the Kirchhoff law. In its usual version, the Kirchhoff law relates the emitted power in a given direction, polarization and frequency to the absorptivity and the blackbody radiance. The derivation of Kirchhoff law is based on the Fluctuation-Dissipation theorem which is valid for local thermodynamic equilibrium [3]. Under continuous pumping, it has been shown that the distribution is no longer a Fermi-Dirac distribution [2], so that the validity of Fluctuation-Dissipation relation is under question. Here, we first derive a non-equilibrium Fluctuation-Dissipation relation which connects the electronic current density fluctuations in a metal with the non-equilibrium distribution. This enables us to derive a generalized form of the Kirchhoff law valid for this non-equilibrium situation. We will also provide a simple physical picture associated with this model.

To conclude, we show that this model allows to explain the main experimental features of photoluminescence. In particular, we recover the spectral modification of the signal as a function of the incident frequency and the nanostructure plasmonic resonance [4]. The model also accounts for the temperature dependence of the photoluminescence which has been used as a temperature sensor in [5]. Finally, we show that the signal is proportional to the pump intensity, in contrast to blackbody radiation. Beyond these theoretical considerations, we confront our model to experimental results presented in detail in a separate contribution at this conference. All in all, these results make a general framework to quantitatively analyze photoluminescence of metal in the cw regime.

References

[1] Mooradian, A. (1969). *Physical Review Letters*, *22*(5), 185.
[2] Sivan, Y., & Dubi, Y. (2021). *ACS nano*, *15*(5), 8724-8732.
[3] Greffet, J. J., Bouchon, P., Brucoli, G., & Marquier, F. (2018). *Physical Review X*, *8*(2), 021008.
[4] Lin, K. Q., Yi, J., Hu, S., Sun, J. J., Zheng, J. T., Wang, X., & Ren, B. (2016). *Acs Photonics*, *3*(7), 1248-1255.
[5] Carattino, A., Caldarola, M., & Orrit, M. (2018). *Nano letters*, *18*(2), 874-880.

Distinguishing thermal from non-thermal ("hot") carriers in illuminated molecular junctions

Yonatan Dubi[1], **Ieng Wai Un**[2], **Yonatan Sivan**[2]

1. Department of Chemistry, Ben-Gurion University; 2. School of Electrical and Computer Engineering, Ben-Gurion University

E-mail: sivanyon@bgu.ac.il

When a plasmonic nanostructure is continuously illuminated, the system unavoidably heats up, and non-thermal (so-called "hot") carriers are being generated. Under continuous wave illumination, the information about heating is characterized by a Fermi-like distribution of carriers close to the Fermi level, whereas the non-thermal carriers reside further away from the Fermi level in nearly-flat "shoulders" [1]. The separation between these different carriers is very challenging, because the number of the high excess-energy non-thermal electrons is many orders of magnitude smaller compared to the number of thermal (i.e., low excess energy) carriers. In an attempt to circumvent this problem, Reddy, Wang and co-authors [2] suggested measuring directly the non-thermal carrier distribution by coupling a plasmonic Au film to a molecular junction. By measuring the I-V curves through the molecular junction (MJ) under illumination and in the dark, they assessed the effect of illumination on the electronic distribution in the illuminated Au electrode.

Here [3], we interpret the results of [2]. Specifically, we extend the theory of transport through a MJ coupled to two electrodes, by combining the standard Landauer theory of transport through MJs and the analytic form for the electron non-equilibrium distribution of an illuminated metal [1]. Using this formulation, we demonstrate that the main results in [2] have a satisfactory explanation as mere heating of the bottom electrode, whereas additional measurements of a different molecule (discussed in the SI of [2]) provides (probably for the first time) a direct observation of non-thermal electrons, but not in the way interpreted in the original manuscript. This finding confirms the original theoretical prediction [1] in a reasonable quantitative manner, and thus confirms the claims on the extremely small role played by non-thermal electron in plasmon-assisted photocatalysis experiments.

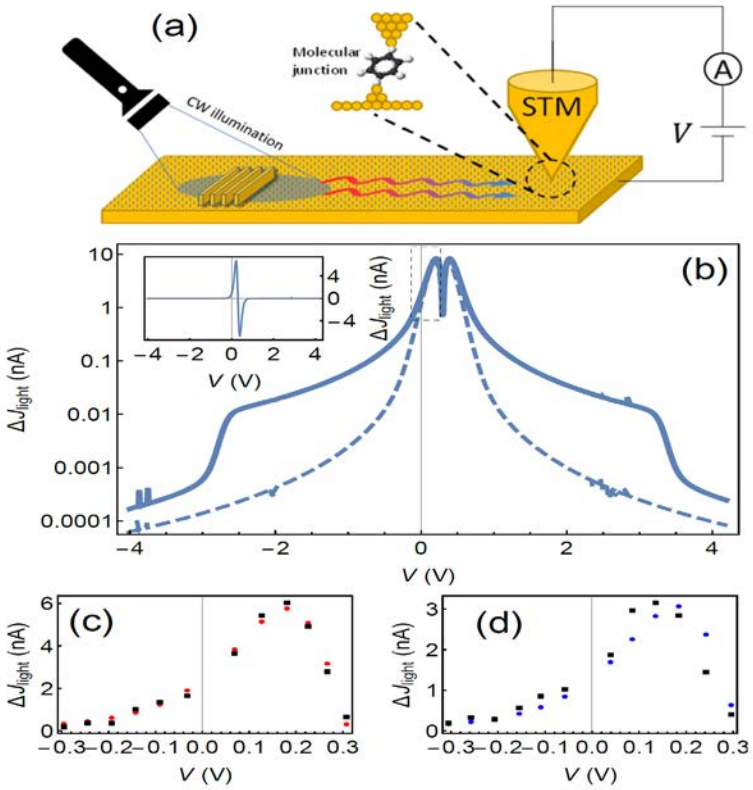

Fig. 1 (a) Schematic depiction of the experimental setup, comprising an Au slab with surface plasmons ecited at the nanofabricated gratings, and a molecular junction formed between the slab and an STM tip. (b) Differential current as a function of bias voltage (log scale) for a molecular junction with resonance close to the Fermi level. The dashed line shows the differential current without illumination, thus showing only the thermal response. Near zero bias (dashed black square), the dominant feature is the thermal contribution to the current, marking that nonthermal effects are negligible there. Inset: same plot in linear scale. (c–d) Fits to experimental data of [2] (c) 6 nm and (d) 13 nm thick slabs, assuming that the tip is not heated but the slab right under it is. Red and blue circles are the experimental data, and black squares are the fits.

References

[1] Dubi, Y., Sivan, Y., (2019*) Light: Science & Applications*, 8, 89-95.
[2] Reddy, H. *et al*. (2020) *Science*, 369, 423–426.
[3] Dubi, Y., Un, I.W., Sivan, Y., (2022*) Nano Letters*, in Print.

Far-field wavefront optimization of the near-field of disordered plasmonic metasurfaces

Gauthier Roubaud[1], Sébastien Bidault[1], Sylvain Gigan[2], Samuel Gresillon[1]

1. Institut Langevin, ESPCI Paris, Université PSL, CNRS, 75005 Paris, France
2. Laboratoire Kastler Brossel, ENS, CNRS, Sorbonne Université, PSL University, 24 rue Lhomond, 75005 Paris

E-mail : samuel.gresillon@espci.fr

Plasmonic nanoantennas featuring nanoscale gaps can exhibit strongly enhanced optical near-fields that have been extensively used in surface enhanced spectroscopy (Raman and Fluorescence) and in biosensing. However, deterministic nanostructures do not provide numerous degrees of freedom to control optically these local field enhancements. By comparison, wavefront shaping techniques in disordered scattering media provide numerous degrees of freedom to control light focusing in space and time [1]. To associate local field enhancements and far-field wavefront control, we use disordered plasmonic surfaces close to the percolation threshold that feature both hotspots [2] and delocalized plasmon modes that can be controlled using a spatial light modulator [3].

In this presentation, we demonstrate how controlling the phase of an incoming femtosecond pulsed laser on a disordered gold surface allows us to optimize the two-photon induced luminescence (TPL) at a chosen position. Importantly, the TPL signal has been shown to provide a far-field image of local field enhancements in nanoantennas [4]. Our results therefore indicate a far-field optimization of the optical near-field in disordered plasmonic metasurfaces.

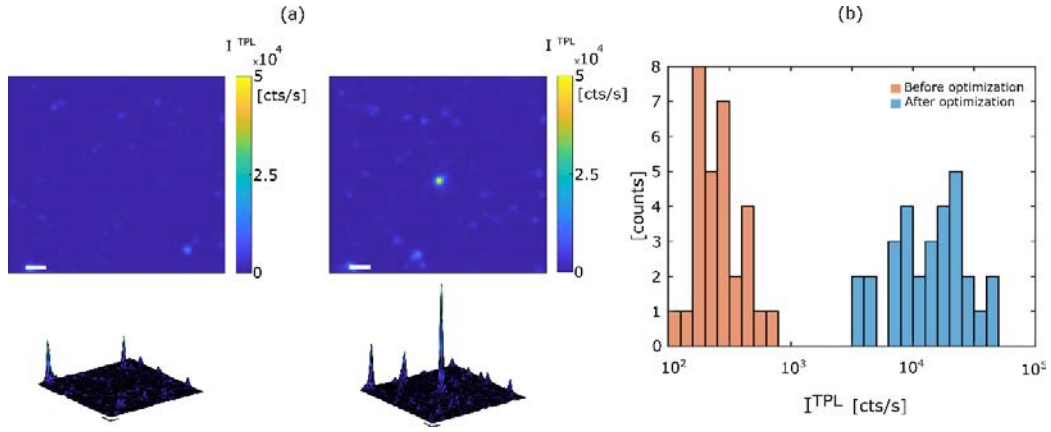

Fig. 1 (a) Widefield Two Photon Luminescence images of the gold metasurface before (left) and after (right) the optimization process; with a strong increase of the TPL signal in the centre of the image after optimization. (b) Distributions of TPL signals before (orange data points) and after optimization (blue) for 30 different optimization experiments.

In practice, the surface of a spatial light modulator is conjugated with the sample plane using a high numerical aperture inverted microscope in order to spatially modulate the phase of the incoming femtosecond source while preserving a homogeneous intensity. The emitted TPL is then imaged in parallel on a CMOS camera. A random optimization process of the incoming wavefront is then performed in order to enhance the TPL signal at the centre of the image (see Fig. 1-a).

Fig. 1-b presents the distribution of TPL signals before and after optimization for 30 different realizations with a typical two orders of magnitude enhancement of the measured signal. These results demonstrate a strong enhancement of the nonlinear luminescence at any chosen position of the sample, at the diffraction limit; indicating an optimization of the near-field in disordered plasmonic metasurfaces by far-field wavefront shaping[5,6].

References

[1] M. Mounaix, D. Andreoli, H. Defienne, G. Volpe, O. Katz, S. Grésillon, and S. Gigan, "Spatiotemporal Coherent Control of Light through a Multiple Scattering Medium with the Multispectral Transmission Matrix", Phys. Rev. Lett. 116, 253901 (2016).
[2] S. Grésillon L. Aigouy, A. C. Boccara, J. C. Rivoal, X. Quelin, C. Desmarest, P. Gadenne, V. A. Shubin, A. K. Sarychev, and V. M. Shalaev, "Experimental Observation of Localized Optical Excitation in Random Metal-Dielectric Films", Phys. Rev. Lett. 82, 4520 (1999).
[3] P. Bondareff, G. Volpe, S. Gigan and S. Gresillon, "Probing Extended Modes on Disordered Plasmonic Networks by Wavefront Shaping", ACS Photonics 2, 12, 1658 (2015).
[4] P. Ghenuche, S. Cherukulappurath, T. H. Taminiau, N. F. van Hulst, and R. Quidant, "Spectroscopic Mode Mapping of Resonant Plasmon Nanoantennas", Phys. Rev. Lett. 101, 116805 (2008).
[5] G. Roubaud, P. Bondareff, G. Volpe, S. Gigan, S Bidault and S. Gresillon, "Far-Field Wavefront Control of Nonlinear Luminescence in Disordered Gold Metasurfaces", Nanoletters 20, 2291 (2020).
[6] G. Roubaud, S. Bidault, S. Gigan and S. Gresillon, "Statistical Nonlinear Optical Mapping of Localized and Delocalized Plasmonic Modes in Disordered Gold Metasurfaces", ACS Photonics 8, 1973 (2021).

Tuning surface lattice resonance energy levels and their degeneracy by breaking isotropy of nanoparticles arrays

Florian Lamaze[1], William D'Orsonnens[1], Julien Proust[1], Louis Giraudet[2]

1. Light, nanomaterials, nanotechnologies EMR 7004, Université de Technologie de Troyes, 10004 Troyes
2. Laboratoire De Recherche en Nanosciences (LRN) - EA 4682, Université de Reims Champagne-Ardenne, 51687 Reims
E-mail: florian.lamaze@utt.fr

The study of plasmonic nanoparticles arrays has led to the observation of the well-known Surface Lattice Resonance (SLR). They appear from the diffraction coupling at specific wavelengths, associated with the appearance or disappearance of a diffraction order [1]. The resulting wave is able to propagate parallel to the array, at a grazing angle. This phenomenon is known as the Rayleigh anomaly and is linearly dependent on the period. This propagating wave thus provides long-distance coupling between the individual nanoantennas along the propagation direction of the diffracted order. In these conditions, a hybridization between the resonance associated with the Rayleigh anomaly and the localized plasmon resonance is supported by the nanoantennas. As such, these period dependent anomalies can be modulated by acting on the geometry of the structure.

In this talk, we will describe and study these resonances for various shapes of particles, both experimentally and with Finite Difference Time Domain (FDTD) simulations, to exploit their specific properties and different responses in polarization. These variety of shape will be investigated for different configuration of arrays. We used electron beam lithography to fabricate the structure on solid substrate, as shown on the SEM image on Fig.1 (b), and then transferred on a flexible substrate with a homemade process.

In particular, it is possible to remove the degeneracy existing between the diffracted orders (±1.0) and (0.±1) in the case of a square array by making it asymmetrical [2], for example by applying a deformation. We then obtain two Rayleigh anomalies, each depending on a distinct period and moving respectively towards the lowest and highest energies levels as shown on Fig 1 (c,d).

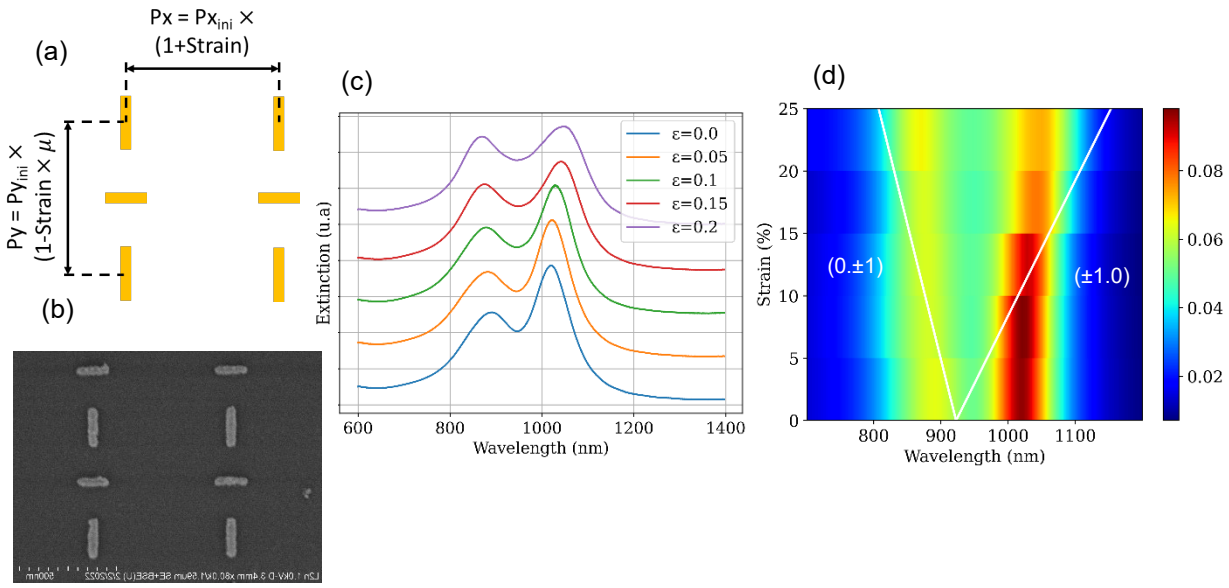

Fig. 1 (a) Schematic of the structure consisting of an array of gold nanorods. (b) SEM image of the structure. (c) Experimental extinction spectra of the array for different deformation state. (d) Experimental extinction map for different deformation state with the associated Rayleigh anomalies.

References

[1] Khlopin, D. Laux, F. Wardley, W.P. Martin, J, Wurtz, G.A., Plain, J. Bonod, N. Zayats, A.V. Dickson, W and Gerard, D. 2017. *J Opt Soc Am B*, 3(34), 691-700.
[2] Guo, R. Hakala, T.K. and P. Törmä. 2017. *Phys. Rev. B*, 95(15), 155423.

Optical antennas driven by inelastic tunnel junctions

Kai Braun*[1], Michel Rebmann[1] and Alfred J. Meixner[1]

1. Institute of Physical and Theoretical Chemistry, University of Tuebingen, Auf der Morgenstelle 18, 72076 Tuebingen and LISA+, Germany
E-mail: kai.braun@uni-tuebingen.de

The conversion of an electrical signal to an optical signal with maximum bandwidth and practical on-chip integration is of fundamental interest. Therefore, light emission by inelastic tunneling has gained considerable interest, since it allows to construct an electrically driven plasmonic nano gap antenna. Accurate control of the shape, aspect ratio, and gap size of the structures determines the spectral shape[1], position, and width of the plasmonic resonances[2]. Many emerging nano-photonic technologies depend on the careful control of such localized resonances, including optical nano antennas for high-sensitivity sensors, nanoscale control of active devices[3], and improved photovoltaic devices.

However, achieving reproducible and stable experimental conditions with nanometer sized gaps in tunneling range remains a challenging task in high demand. We have investigated different approaches to establish these conditions. Ether, by an gold tip positioned in tunneling range above an gold samples, to produce a gap mode antenna, which can be driven by an applied bias voltage, or by fabricated arrays of vertical coupled antennas in metal-insulator-metal arrangements. These IET devices are based on electrically connected gold nano rods (GNR) and hexagonal boron nitride as insulating layer. By tuning the aspect ratio of the GNRs we shift the localized plasmon resonance of the antennas and adjust the emission wavelength. Secondly, we used

The results discussed here show solutions of antenna modulated light emission from a tunneling junction approaching the ultimate size limits of an opto-electronic device, while the operating speed is only limited by the electron tunneling time. The reviewed concept represents a novel platform for ultra-small, fast, optically, and electronically switchable devices.

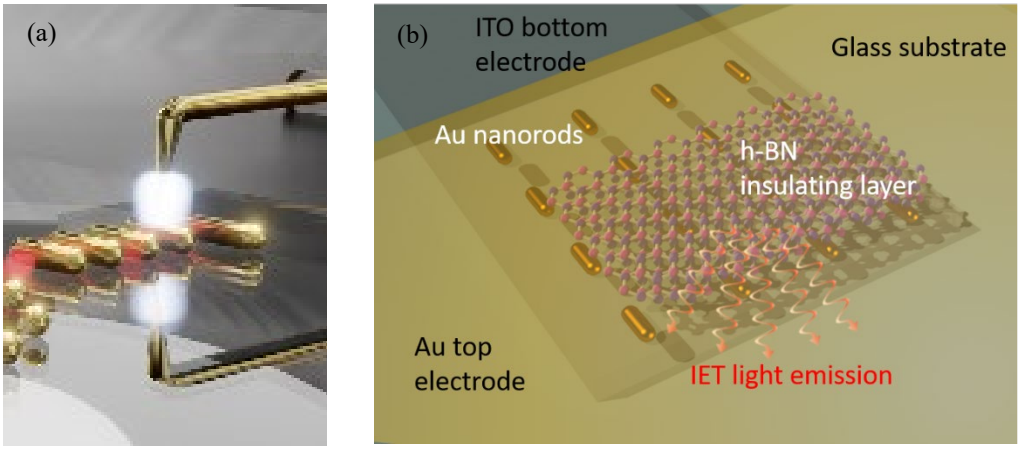

Fig. 1 Different approaches to establish plasmonic tunnel junctions. (a) A STM tunneling junction on a plasmonic particle and (b) a stacking device, starting with an ITO bottom electrode on glass, followed by an array of GNRs. Afterwards a few layers sheet of h-BN is transferred, and an evaporated Au top electrode complete the device. Electrons tunnel from the Au top electrode to the GNRs, where inelastic tunneling occurs and transfers energy to the plasmon, which later determines the emission wavelength

References

[1] Mühlschlegel, P., Eisler, H.J., Martin, O. J. F. et al. „Resonant Optical Antennas“ Science 308, 1607-1609, 2005
[2] Kern J., Grossmann J., B. Hecht et al. „Atomic-Scale Confinement of Resonant Optical Fields” Nano Letters, 12, 5504, 2012
[3] Braun K., Laible F., Wang X., et al. “Active optical antennas driven by inelastic electron tunneling” Nanophotonics, 7 (9), 1503, 2018

Generating ultrafast stationary magnetic fields with light in a plasmonic nanostructure

Mathieu Mivelle[1], Xingyu Yang[1], Ye Mou[1], Bruno Gallas[1], Agnès Maitre[1], Laurent Coolen[1]

1. Sorbonne Université, CNRS, Institut des NanoSciences de Paris, INSP, F-75005 Paris, France

E-mail: mathieu.mivelle@sorbonne-universite.fr

The inverse Faraday effect allows the generation of stationary magnetic fields through optical excitation only [1]. This light-matter interaction in metals results from creating drift currents *via* non-linear forces that light applies to the conduction electrons. Here, we theoretically demonstrate that a gold photonic nano-antenna, optimized by a genetic algorithm, allows, under high excitation power, to maximize the drift currents and generate a pulse of stationary magnetic fields in the tesla range [2] (fig. 1). This intense magnetic field, confined at the nanoscale and for a few femtoseconds, results from annular optical confinement and not from the creation of a single optical hot spot. Moreover, by controlling the incident polarization state, we demonstrate the orientation control of the created magnetic field and its reversal on demand. Finally, the stationary magnetic field's temporal behavior and the drift currents associated with it reveal the sub-cycle nature of this light-matter interaction. The manipulation of drift currents by a plasmonic nanostructure for the generation of stationary magnetic field pulses find applications in the ultra-fast control of magnetic domains with applications in data storage technologies, but also in research fields such as magnetic trapping, magnetic skyrmion, magnetic circular dichroism, to spin control, spin precession, spin currents, and spin-waves, among others.

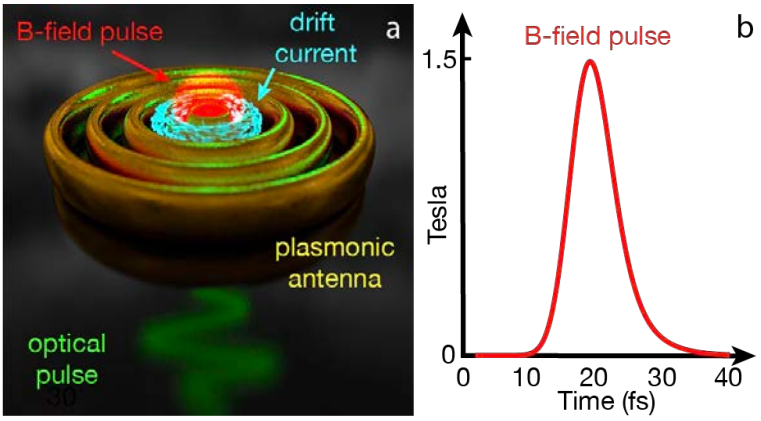

Fig. 1. a) A genetically-designed plasmonic nanostructure excited by a femtosecond pulse of light (green oscillations) sets the electrons of the metal (symbolized by the blue sparks) in a drift motion, generating a stationary magnetic field of a few Tesla at the nanoscale (red halo) and b) of only a few femtoseconds [2].

References

[1] Van Der Ziel, J.; Pershan, P. S.; Malmstrom, L. 1965. *Phys. Rev. Lett.*, 15, 190.

[2] Yang, X.; Mou, Y.; Gallas, B.; Maitre, A.; Coolen, L.; Mivelle, M.; 2021. *ACS nano.*,16, 386-393.

Spectroscopic Mapping of Plasmonic Dynamics on the Surface of Nanoparticle Plasmonic Particles

Derek B. Nowak[1], **Padraic O'Reilly**[1]
1. Molecular Vista Inc, 6840 Via Del Oro Suite 110, San Jose CA
E-mail: derek@molecularvista.com

The study of plasmonic particle absorption and scattering behavior has been ongoing for centuries. In more recent times the role that localized surface plasmon resonances (LSPR) play in this understanding has been demonstrated mathematically through analytical and numerical modeling, and experimentally through the far-field response of plasmonic nanoparticles either individually isolated or in ensembles using a variety of spectroscopic and microscopic techniques. Moreover, near-field studies have further confirmed our understanding of the optical response of nanoscale particles using scattering scanning near-field optical microscopy (sSNOM), two photon-induced luminescence (TPL) microscopy and electron energy loss spectroscopy (EELS). Where these techniques have been successful is allowing researchers to map the field distributions at the nanoscale, there are still some challenges. For s-SNOM the strong background scattered light component limits the signal to noise ratio of the system [1], it is also challenging to change the wavelength of excitation in real-time and provide a spectrum of the plasmonic response of the particles. For TPL the spatial resolution tends to be lower in comparison to tip based techniques [2]. For EELS, while it fares better for spatial resolution, the limitations in sample compatibility, sample charging, and sample alterations require experimental consideration [3]. Ideally a technique that probes the absorption behavior at the intra-particle level will lead to information about how these nanoparticles interact with their local environment, which would have far-reaching impact in the areas of biomedical technologies, renewable energy, plasmon-enhanced spectroscopies, and optoelectronic devices, to name a few. An emerging new near-field detection method based on optical force, photo-induced force microscopy (PiFM) was used first by Halas group at Rice University to investigate LSPRs and showed some initial promise in this direction [4]. A critical element that is needed is the capability to tune the excitation visible light source to provide a local spectroscopic measurement. Recent developments with the combination of PiFM with supercontinuum light sources have now made this type of spectroscopic measurement routinely possible [5].

To demonstrate the spectroscopic capabilities of the PiFM detection mechanism we use the output of a supercontinuum laser source focused onto the imaging apex of a metal coated AFM cantilever. An acoustic optical tunable filter is used to spectrally filter the output of the of this white light source, controlling both the linewidth and center output wavelength electrotonically. We can observe local intra-particle variation in absorption spectrum present on the surface of nanoparticles as shown in Fig 1. These results correspond to the expected results from absorption experiments [6] and mathematical modeling. PiFM demonstrates a promising method to study intraparticle absorption dynamics and how these particles interact in their local environments. Moreover, these spectroscopic measurements are acquired simultaneously with topography from the AFM probe, providing a direct correlation with morphology of the nanoparticle and local environment.

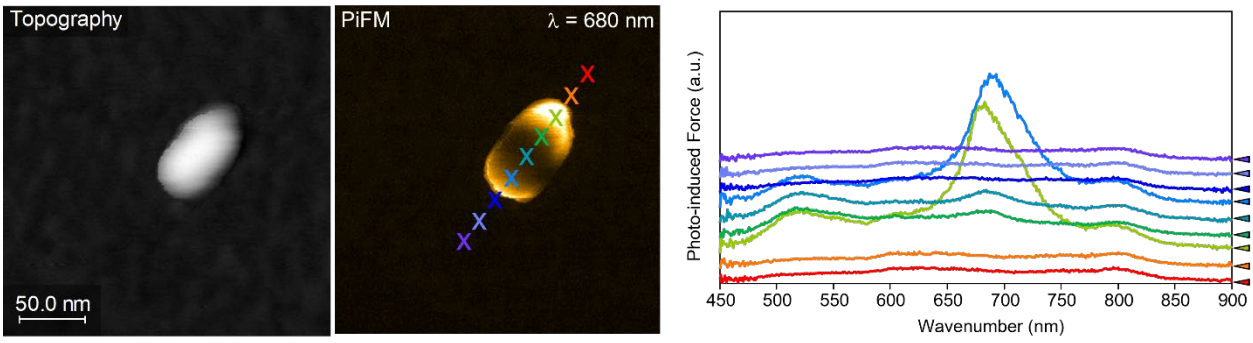

Fig. 1 A single Au nanorod is imaged using a metallic AFM cantilever (left) while a simultaneous PiFM image is acquired with a fixed excitation wavelength of 680 nm (center). A set of spectra acquired across the nanorod shows clearly the longitudinal (690 nm) and transverse modes (525 nm) of the nanorod as measured near the surface of the particle.

References

[1] Xiao, L.; Schultz, Z. D. *Anal. Chem.* **2018,** *90* (1), 440-458
[2] Chen, L.; Li, G.; Liu, G.; Dai, Q.; Lan, S.; Tie, S.; Deng, H. *J. Phys. Chem. C* **2013**, 117(39), 20146-20153.
[3] Liang, H.; et.al. *J. Am. Chem. Soc.* **2013**, 135(26), 9616-9619.
[4] Tumkur, T. U.; Yang, X.; Cerjan, B.; Halas, N. J.; Nordlander, P.; Thomann, I. *Nano Lett.* **2016,** *16* (12), 7942-7949.
[5] D. Nowak, (2022) Spectroscopic and High-Resolution Microscopic Characterization of Intra-Nanoparticle Plasmonic Absorption Dynamics at Visible Wavelengths (Manuscript in preparation), Molecular Vista Inc.
[6] Muskens, O. L.; et. al. *Appl Phys Lett* **2006**, 88, 063109.

Acousto-Plasmonic Coupling: The Raman Energy Density (RED)

Nicolas Large[1], **Jose Luis Montaño-Priede**[1], **Adnen Mlayah**[2,3]

1. Department of Physics & Astronomy, University of Texas at San Antonio, One UTSA Circle, San Antonio, Texas 78249, United States
2. Centre d'Elaboration de Matériaux et d'Etudes Structurales, CNRS – Université de Toulouse, 29 Rue J. Marvig, 31055 Toulouse, France
3. Laboratoire d'Analyse et d'Architecture des Systèmes, CNRS – Université de Toulouse, 7 avenue du Colonel Roche, 31031 Toulouse, France

E-mail: Nicolas.Large@utsa.edu

Interactions between elementary excitations, such as plasmon-exciton and plasmon-phonon, are of great interest from a fundamental point of view and for applications. While plasmon-exciton interactions have been extensively studied both experimentally and theoretically [1], the interaction mechanisms between acoustic vibrations (phonons) and localized surface plasmons (LSPs) remain largely unexplored [2]. Here we present a theoretical investigation of the interactions between confined acoustic vibrations and LSPs in the framework of resonant acoustic Raman scattering. We express the Raman scattering process in the framework of Fermi golden rule and introduce for the first time the concept of Raman energy density (RED). Similarly to the Raman-Brillouin electronic density (RBED) introduced for semiconductors [3–4], this new physical quantity is used as a theoretical tool for the interpretation of resonant Raman scattering mediated by LSPs in metallic nanoparticles. The RED represents the electromagnetic energy density excited by the Raman probe and modulated by the acoustic vibrations of the nanoparticle. We show that, similarly to the local density of optical states (LDOS) and the RBED, the RED is a local physical quantity that can be mapped in the near-field region. It provides a clear picture of the interaction between LSPs and acoustic vibrations which give rise to inelastic scattering measurable in the far-field. Here, we use the newly introduced RED concept to investigate elastic (an)isotropy effects and calculate the Raman selection rules of spherical nanoparticles in a dielectric environment.

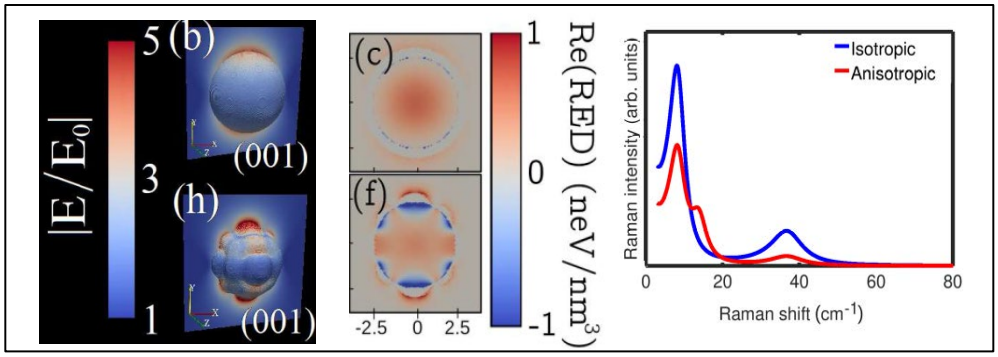

Fig. 1 Left: Isotropic (l=0) and Anisotropic (A_{1g}) breathing acoustic mode of a AuNP modulating the near electric field induced par the dipolar localized surface plasmon (LSP). Center: Raman energy density (RED) resulting from the interaction of the l=0 and A_{1g} vibration mode with the dipole LSP. Right: Calculated acoustic Raman spectra for the isotropic and anisotropic nanoparticles.

References

[1] Schlather, A. E.; Large, N.; Urban, A. S.; Nordlander, P. and Halas, N. J. "Near-Field Mediated Plexcitonic Coupling and Giant Rabi Splitting in Individual Metallic Dimers," *Nano Lett.,* 2013, 13, 3281

[2] Large, N.; Saviot, L.; Margueritat, J.; Gonzalo, J.; Afonso, C. N.; Arbouet, A.; Langot, P.; Mlayah, A. and Aizpurua, J. "Acousto-plasmonic Hot Spots in Metallic Nano-Objects," *Nano Lett.,* 2009, 9, 3732

[3] Large, N.; Huntzinger, J. R..; Aizpurua, J.; Jusserand, B. and Mlayah, A. "Raman-Brillouin electronic density in short period superlattices," *Phys. Rev. B,* 2010, 82, 075310

[4] Mlayah, A.; Huntzinger, J.-R. and Large, N. "Raman-Brillouin light scattering in low-dimensional systems: Photoelastic model versus quantum model," *Phys. Rev. B,* 2007, 75, 245303